

The fumarolic CO₂ output from Pico do Fogo volcano (Cape Verde)

Journal:	<i>Italian Journal of Geosciences</i>
Manuscript ID	IJG-2020-0838.R1
Manuscript Type:	Original Article
Date Submitted by the Author:	n/a
Complete List of Authors:	<p>Aiuppa, Alessandro; Università di Palermo Dipartimento di Scienze della Terra e del Mare, Bitetto, Marcello; Università di Palermo Dipartimento di Scienze della Terra e del Mare Rizzo, Andrea; Istituto Nazionale di Geofisica e Vulcanologia Sezione di Palermo Viveiros, Maria; Instituto de Investigação em Vulcanologia e Avaliação de Riscos Allard, Patrick; Institut de Physique du Globe de Paris Frezzotti, Maria Luce; Università degli Studi di Milano-Bicocca Dipartimento di Scienze dell'Ambiente e del Territorio e di Scienze della Terra Valenti, Virginia; Università degli Studi di Milano-Bicocca Dipartimento di Scienze dell'Ambiente e del Territorio e di Scienze della Terra Zanon, Vittorio; Instituto de Investigação em Vulcanologia e Avaliação de Riscos</p>
Keywords:	Pico do Fogo volcano, Cape Verde, volcanic gases, CO ₂ output

SCHOLARONE™
Manuscripts

The fumarolic CO₂ output from Pico do Fogo volcano (Cape Verde)

Alessandro Aiuppa^{1,*}, Marcello Bitetto¹, Andrea L. Rizzo², Fatima Viveiros³,

Patrick Allard⁴, Maria Luce Frezzotti⁵, Virginia Valenti⁵, Vittorio Zanon^{3,4}

¹*Dipartimento DiSTeM, Università di Palermo, Italy*

²*Istituto Nazionale di Geofisica e Vulcanologia, Sezione di Palermo, Italy*

³*Instituto de Investigação em Vulcanologia e Avaliação de Riscos, University of the Azores, Portugal*

⁴*Institute de Physique du Globe de Paris, Université de Paris, France*

⁵*Dipartimento di Scienze dell'Ambiente e della Terra, Università di Milano Bicocca, Italy*

*Corresponding author: alessandro.aiuppa@unipa.it

ABSTRACT

Pico do Fogo volcano, in the Cape Verde archipelago off the western coasts of Africa, has been the most active volcano in the Macaronesia region in the Central Atlantic, with at least 27 eruptions during the last 500 years. Between eruptions fumarolic activity has been persisting in its summit crater, but limited information exists for the chemistry and output of these gas emissions. Here, we use the results acquired during a field survey in February 2019 to quantify the quiescent summit fumaroles' volatile output for the first time. Combining measurements of the fumarole compositions (using both a portable Multi-GAS and direct sampling of the hottest fumarole) and of the SO₂ flux (using near-vent UV Camera recording), we quantify a daily output of 1060±340 tons CO₂, 780±320 tons H₂O, 6.2±2.4 tons H₂S, 1.4±0.4 tons SO₂ and 0.05±0.022 tons H₂. We show that the fumarolic CO₂ output from Pico do Fogo exceeds (i) the time-averaged CO₂ release during 2015-type recurrent eruptions and (ii) is larger than current diffuse soil degassing of CO₂ on Fogo Island. When compared to worldwide volcanoes in quiescent hydrothermal-stage, Pico do Fogo is found to rank among the strongest CO₂ emitters. Its substantial CO₂ discharge implies a continuous deep

1
2
3 27 supply of magmatic gas from the volcano's plumbing system (verified by the low but measurable
4
5 28 SO₂ flux), that becomes partially affected by water condensation and sulphur scrubbing in fumarolic
6
7
8 29 conduits prior to gas exit. Variable removal of magmatic H₂O and S accounts for both spatial
9
10 30 chemical heterogeneities in the fumarolic field and its CO₂-enriched mean composition, that we
11
12 31 infer at 64.1±9.2 mol. % H₂O, 35.6±9.1 mol. % CO₂, 0.26±0.14 mol. % total Sulfur (S_t), and
13
14 32 0.04±0.02 mol. % H₂.

15
16
17 33
18
19 34 **Keywords:** *Pico do Fogo volcano; Cape Verde, volcanic gases, CO₂ output*

20 21 35 22 23 24 36 INTRODUCTION

25
26 37 Together with tectonic degassing, subaerial volcanism is the primary outgassing mechanism of
27
28 38 mantle-derived CO₂ to the atmosphere (WERNER *et alii*, 2019; FISCHER *et alii*, 2019). Over
29
30 39 geological time, tectonic and volcanic degassing have been the primary mechanisms for carbon
31
32 40 exchange in and out our planet (DASGUPTA AND HIRSCHMANN, 2010; DASGUPTA, 2013; WONG *et*
33
34 41 *alii*, 2019), ultimately playing a control role on pre-industrial atmospheric CO₂ levels and the
35
36 42 climate (VAN DER MEER *et alii*, 2014; BRUNE *et alii*, 2017). Although attempts to estimate the global
37
38 43 volcanic CO₂ output started early back in the 1990s (e.g., GERLACH, 1991), substantial budget
39
40 44 refinements have only recently arisen from the 8-years (2011-2019) DECADE (Deep Earth Carbon
41
42 45 Degassing; <https://deepcarboncycle.org/about-decade>) research program of the Deep Carbon
43
44 46 Observatory (<https://deepcarbon.net/project/decade#Overview>) (FISCHER, 2013; FISCHER *et alii*,
45
46 47 2019).

47
48 48 One key result of DECADE-funded research has been the recognition that the global CO₂ output
49
50 49 from subaerial volcanism is predominantly sourced from a relatively small number of strongly
51
52 50 degassing volcanoes. AIUPPA *et alii*, (2019) showed that the top 91 SO₂ volcanic emitters in 2005-
53
54 51 2015 (those systematically detected from space; CARN *et alii*, 2017) produce a cumulative CO₂
55
56 52
57
58
59
60

1
2
3
4
5
6
7
8
9
10
11
12
13
14
15
16
17
18
19
20
21
22
23
24
25
26
27
28
29
30
31
32
33
34
35
36
37
38
39
40
41
42
43
44
45
46
47
48
49
50
51
52
53
54
55
56
57
58
59
60

release of ~39 Tg/yr, nearly half of which (~19 Tg CO₂/yr) is produced by only 7 top-degassing volcanoes. It has also been found, however, that a non-trivial CO₂ output is additionally sustained by fumarolic degassing (FISCHER *et alii*, 2019; WERNER *et alii.*, 2019) and groundwater transport (TARAN, 2009; TARAN AND KALACHEVA, 2019) at hydrothermal volcanoes in quiescent stage. These low-temperature (hydrothermal) fumarolic emissions typically release CO₂ in the absence of easily detectable (by Ultra Violet (UV) spectroscopy) SO₂, implying that traditional “indirect” CO₂ flux quantification using the volcanic gas CO₂/SO₂ ratio proxy in tandem with remotely sensed SO₂ fluxes (e.g. WERNER *et alii*, 2019) cannot be employed; more challenging airborne (WERNER *et alii*, 2009) or ground-based (PEDONE *et alii*, 2014; AIUPPA *et alii*, 2015; QUEIBER *et alii*, 2016) “direct” CO₂ flux measurements are required instead. These technical limitations have prevented us from establishing a robust catalogue for fumarolic CO₂ outputs, as <50 of the several hundred degassing volcanoes in “hydrothermal-stage” worldwide have been measured for their CO₂ flux (WERNER *et alii*, 2019). As a consequence, the extrapolated current inventories for the global fumarolic hydrothermal CO₂ flux (from 15 to 35 Tg CO₂/yr; FISCHER *et alii*, 2019; WERNER *et alii*, 2019) still involve very large uncertainties. In addition, most of the available information is for low-temperature arc volcanic gases, while much less is known for the fumarolic CO₂ output for non-arc settings (divergent, intra-plate or continental rift; e.g., ILYINSKAYA *et alii*, 2015, 2018).

Pico do Fogo, in the Cape Verde archipelago, makes part of the Macaronesia region, an area of the Atlantic Ocean off the western coasts of Africa also including the archipelagos of the Azores, Madeira and Canary (Fig. 1). This 2829 m a.s.l high strato-volcano (Fig. 2a), located on the island of Fogo, has been the most frequently erupting volcanic centre of the Macaronesia region in the last 500 years (RIBEIRO, 1960). All historical eruptions occurred on its upper flanks or in its summit crater. Between eruptions, the summit crater of Pico do Fogo hosts a persistent fumarolic field (Fig. 2b-e), with several gas vents ranging in temperature from boiling to >200°C (DIONIS *et alii*, 2014; MELIÁN *et alii*, 2015). The CO₂ output sustained by diffuse degassing across the crater floor was

1
2
3 77 estimated in the range 147 ± 35 (in 2009) to 219 ± 36 t/d (in 2010) (DIONIS *et alii*, 2014, 2015), but no
4
5 78 comparable data yet exists for the fumarolic CO₂ output itself.
6
7

8 79 Here we fill this gap of knowledge by presenting the very first results for the fumarolic output of
9
10 80 CO₂ and other volatiles from Pico do Fogo. These results were obtained from a gas survey on
11
12 81 February 5, 2019, during which we combined real-time in-situ measurement of the crater gas
13
14 82 compositions (Multi-GAS), direct sampling of the hottest fumarole, and near-vent remote sensing of
15
16 83 the SO₂ flux with an UV Camera. Our new data set contributes to improved quantification and
17
18 84 understanding of Fogo's quiescent degassing during the multi-decadal phases separating eruptions,
19
20 85 and offers an interesting comparison with the gas output measured during the recent 2014-2015
21
22 86 eruption (HERNÁNDEZ *et alii*, 2015). More broadly, our results for Pico do Fogo add a novel piece
23
24 87 of information to the still fragmentary data base for fumarolic CO₂ emissions from global volcanoes
25
26 88 in hydrothermal stage.
27
28
29
30
31
32

33 90 **FOGO ISLAND AND PICO DO FOGO VOLCANO**

34
35 91 The Cape Verde archipelago, extending between 15 and 17°N latitude 500 km to the west of
36
37 92 Senegal, is composed of 10 main islands that are the emerged portions of a high oceanic plateau (2
38
39 93 km above the sea floor). Fogo Island is located at the south-western edge of this system (Fig. 1).
40
41 94 The Cape Verde oceanic Rise, the world's largest geoid and bathymetric seafloor anomaly
42
43 95 (COURTNEY & WHITE, 1986), has been interpreted as due to a hot-spot mantle swell centred north-
44
45 96 east of the Sal island (CROUGH, 1978, 1982; HOLM *et alii*, 2008). The presence of an active mantle
46
47 97 plume beneath the northern part of Cape Verde at least has been suggested by some authors based
48
49 98 on seismic imaging (MONTELLI *et alii*, 2006; LIU & ZHAO, 2014; SAKI *et alii*, 2015). A mantle
50
51 99 plume contribution is also consistent with high primordial ³He (³He/⁴He ratios up to 12.3-15.7 Ra)
52
53 100 in volcanics from Sao Vicente and Sao Nicolau islands (CHRISTENSEN *et alii*, 2001; DOUCELANCE *et*
54
55 101 *alii*, 2003; MATA *et alii*, 2010; MOURÃO *et alii*, 2012). However, a plume origin for Macaronesian
56
57
58
59
60

1
2
3 102 volcanism is still matter of debate (BONATTI, 1990; ASIMOV *et alii*, 2004), and the role of
4
5 103 decompressional melting (MÉTRICH *et alii*, 2014) favoured by extensional lithospheric
6
7
8 104 discontinuities (MARQUES *et alii*, 2013) has received increased attention recently. Volcanism on the
9
10 105 Cape Verde Islands is thought to have started 24–22 Ma ago on the northeastern islands, followed
11
12 106 by a more recent westward migration of volcanic activity (both in the northern and southern
13
14
15 107 branches of the archipelago) during the Pliocene-Pleistocene (HOLM *et alii*, 2008). Erupted products
16
17 108 spread a large compositional range but mafic, silica-undersaturated lavas (basanites, tephrites, and
18
19 109 nephelinites) prevail (GERLACH *et alii*, 1988; DAVIES *et alii*, 1989; HOLM *et alii*, 2006), eventually
20
21 110 associated with rarer carbonatites (KOGARKO *et alii*, 1992; HOERNLE *et alii*, 2002). Trace-element
22
23
24 111 and isotope geochemistry of the erupted volcanics are extremely heterogeneous, with significant
25
26 112 differences between the northern and southern islands, implying the probable involvement of
27
28 113 several distinct mantle sources: a lower mantle plume containing both mixed HIMU (High
29
30
31 114 $\mu = {}^{238}\text{U}/{}^{204}\text{Pb}$ at zero age) and EM1 (Enriched Mantle 1) end-members, possibly a 1.6-Ga
32
33 115 recycled oceanic crust, plus the depleted upper mantle (northern islands) and the subcontinental
34
35 116 lithospheric mantle (southern islands) (GERLACH *et alii*, 1988; DAVIES *et alii*, 1989; HOLM *et alii*,
36
37 2006; CHRISTENSEN *et alii*, 2001; DOUCELANCE *et alii*, 2003; MILLET *et alii*, 2008). The actual
38 117 relative proportions of each of these sources are still debated however.
39
40 118

41
42 119 Fogo Island (Fig. 1b), formed during the last 3–4.5 Ma, has been the single site of historical
43
44
45 120 volcanic activity (27 reported eruptions) since the discovery of the Cape Verde archipelago in the
46
47 121 XVth century. The dominant structure of the island is Monte Amarelo volcano, whose summit was
48
49 122 truncated by three massive flank collapses between ca. 60 and 43 ka (Fig. 1b) (DAY *et alii*, 1999;
50
51 123 2000; MARQUES *et alii*, 2020). The post-collapse (62 ka to present) activity has been primarily
52
53
54 124 concentrated within the Chã das Caldeiras depression (Fig. 1b), leading to progressive infilling of
55
56 125 the collapse scar and the formation of the Pico do Fogo cone. The cone itself (Fig. 2a) has remained
57
58 126 the primary eruptive centre until 1785 (RIBEIRO, 1960), when fissure-fed effusive eruptions became
59
60

1
2
3 127 concentrated along the flanks of Pico, occurring at an average frequency of one every ~50 years.
4
5 128 The most recent eruptions happened in 1951 (HILDNER *et alii*, 2012), 1995 (HILDNER *et alii*, 2011)
6
7
8 129 and 2014-2015 (CARRACEDO *et alii*, 2015; CAPPELLO *et alii*, 2016; RICHTER *et alii*, 2016; MATA *et*
9
10 130 *alii*, 2017). Eruptive products of the Amarelo-Fogo volcanic complex are primarily alkali-rich
11
12 131 tephritic to basanitic lavas (with rarer foidites and more evolved phonolites). They are thought to
13
14
15 132 ascend from a 16–28 km deep magma storage zone, emplaced in the underlying lithospheric mantle
16
17 133 (GERLACH *et alii*, 1988; DOUCELANCE *et alii*, 2003; HILDNER *et alii*, 2011, 2012; MATA *et alii*,
18
19 134 2017).

24 136 MATERIALS AND METHODS

25
26 137 On February 5, 2019 we realized extensive field investigations and measurements of the summit
27
28 138 crater fumarolic emissions of Pico de Fogo volcano (Fig. 2a-e). We used a portable Multi-
29
30
31 139 component Gas Analyser System (Multi-GAS) to analyse in real-time the fumaroles' compositions
32
33 140 during walking traverses across the fumarolic field (see the track shown in Figure 2e). The walking
34
35 141 traverse mode, first used on Vulcano Island (AIUPPA *et alii*, 2005a), is ideal to explore the chemical
36
37 142 heterogeneity of a fumarolic field as a high number of fumarolic vents can sequentially be analysed
38
39
40 143 while slowly moving along the path. During the traverse, the Multi-GAS continuously acquired data
41
42 144 at 0.5 Hz, and its position was synchronously geo-localized with an embedded GPS. In addition to
43
44
45 145 areas of diffuse soil degassing, 17 main fumarolic vents, showing the strongest emissions, were
46
47 146 identified during the traverse (Fig. 2e). Gas composition at each of these vents was determined
48
49 147 (Tab. 1) by keeping the MultiGAS inlet at a constant position (and for a few minutes) at about ~50
50
51 148 cm height above the fumarolic vent. Our Multi-GAS instrument comprised the following sensor
52
53
54 149 combination (e.g., AIUPPA *et alii*, 2016): a Gascard EDI030105NG infra-red spectrometer for CO₂
55
56 150 (Edinburgh Instruments; range: 0-30,000 ppmv); 3 electrochemical sensors for SO₂ (T3ST/F-
57
58 151 TD2G-1A), H₂S (T3H-TC4E-1A) and H₂ (T3HYT- TE1G-1A), all from City Technology; and a
59
60

1
2
3 152 KVM3/5 Galltec-Mela temperature (T) and relative humidity (Rh) sensor. H₂O concentration in the
4
5
6 153 fumarolic gases was calculated from co-acquired T, Rh and pressure readings using the Arden Buck
7
8 154 equation (see AIUPPA *et alii*, 2016). Reading from the H₂S sensor were corrected for 14% cross-
9
10 155 sensitivity to SO₂. Gas ratios in each of the main fumaroles (Tab. 1) were derived from scatter plots
11
12 156 of the gas concentrations using the Ratiocalc software (TAMBURELLO, 2015). Uncertainties in all
13
14
15 157 derived ratios are <15%, except for H₂O/H₂S ($\leq 25\%$).

16
17 158 The fumarole 15, displaying the highest emission temperature (T = 315°C), was sampled for dry
18
19 159 gases only by inserting a titanium tube 50 cm-long into the vent. This tube was connected to both a
20
21
22 160 quartz line equipped with a condenser in order to remove water vapour and a three-way valve with a
23
24 161 syringe allowing to force gas flow into the line. Three dry gas samples were stored in glass bottles
25
26 162 equipped of two stopcocks and then moved to the INGV laboratory in Palermo for chemical
27
28
29 163 analysis. Concentrations of He, H₂, O₂, N₂, CO, CH₄, CO₂ and H₂S were determined using a gas
30
31 164 chromatograph (Clarus 500, Perkin Elmer) equipped with a 3.5-m column (Carboxen 1000) and a
32
33 165 double detector (hot-wire detector and flame ionization detector [FID]). SO₂ was not measurable
34
35 166 with this sampling/analytical setup. Analytical errors were <3%. The results are reported in Tab. 2.

36
37
38 167 Simultaneously to our Multi-GAS traverse, we also operated a portable dual UV camera system
39
40 168 for measuring the volcanic SO₂ flux. The camera system registered at 0.5 Hz for ~100 minutes from
41
42 169 a fixed position on the inner crater terrace's rim, deep inside the summit crater (see Figs. 2b, 2e).
43
44
45 170 The system used two co-aligned cameras (JAI CM-140GE-UV), both fitted with optical lenses of
46
47 171 45° Field of View, and mounting two different band-pass optical filters with Full Width at Half
48
49 172 Maximum (FWHM) of 10 nm and central wavelengths of 310 and 330 nm, respectively. The filters
50
51
52 173 were applied in front of the cameras so to achieve differential UV absorption in the SO₂ band
53
54 174 (KANTZAS *et alii*, 2009; KERN *et alii*, 2010; DELLE DONNE *et alii*, 2019). The system, housed in a
55
56 175 peli case and powered by a 12V LiPo battery, was mounted on a tripod and rotated to look upward
57
58 176 to image the crater's inner northern slope (where the fumarolic field is located) and a portion of the
59
60

1
2
3 177 background sky (Figs. 2b, 2d). Data acquisition was commanded via PC using the Vulcamera
4
5 178 software (TAMBURELLO *et alii* 2011). The acquired images (520x676 pixels at 10-bit resolution)
6
7
8 179 were post-processed using standard techniques (KANTZAS *et alii*, 2009; TAMBURELLO *et alii*, 2011,
9
10 180 2012): sets of co-acquired images were combined into absorbance images and were then converted
11
12 181 into SO₂ slant column amount (SCA) images by successively using three different calibration cells.
13
14
15 182 Finally, we derived an Integrated Column Amount (ICA) time-series by integrating the SCA along
16
17 183 the cross-section shown in Fig. 2b and then the SO₂ flux by multiplying the ICA with the plume
18
19 184 speed. The plume speed (1.9 ± 0.6 m/s) was obtained by processing image sequences acquired at 0.2
20
21
22 185 Hz using a LifeCam Cinema HD (Microsoft) USB visible camera, integrated in the UV Camera
23
24 186 system. Processing involved quantifying the rising speeds of ~50 individual gas puffs of well-
25
26 187 resolved structure, moving upward from the fumarolic field toward the crater edge (Fig. 2d).

28
29 188 Finally, from the same position as the UV camera, we used a portable handheld thermal camera
30
31 189 (model FLIR E5) in order to acquire a thermal map of the fumarolic field (see Fig. 2b). This map
32
33 190 allowed us to verify that the hottest degassing areas were in large part covered by the Multi-GAS
34
35 191 traverse. Temperatures of fumaroles 5 and 14-15, the hottest vents in the field (Fig. 2b), were also
36
37
38 192 directly measured in situ with a portable thermocouple.

42 194 RESULTS

44 195 FUMAROLIC GAS COMPOSITION: MULTI-GAS AND DIRECT SAMPLING

46
47 196 As a whole, during the ~74-minute duration of our Multi-GAS traverse we obtained 4446
48
49 197 simultaneous measurements of H₂O, CO₂, SO₂, H₂S and H₂ concentrations in Fogo gas emissions
50
51 198 (one analysis every 2 seconds). The entire dataset is illustrated in Figure 3 where the gas
52
53
54 199 concentrations in the near-vent fumarolic plumes are displayed as scatter plots. The concentrations
55
56 200 of H₂O, CO₂ and H₂ were corrected for the respective air background values of ~12,000, ~600 and
57
58 201 ~0.5 ppmv measured upwind (outside) the fumarolic field (Fig. 2e). The high background CO₂
59
60

1
2
3 202 concentration compared to “normal” atmosphere (~400 ppmv) is explained by the high diffuse soil
4
5 203 CO₂ emission through the inner crater floor (DIONIS *et alii*, 2014, 2015).

7
8 204 The absolute gas concentrations measured along our traverse display quite large variations (Fig.
9
10 205 3), indicating chemical heterogeneity in the fumarolic field emissions. This is especially evident in
11
12 206 the SO₂ vs. H₂S scatter plot (Fig. 3). Otherwise, one observes broad co-variations among most gas
13
14 207 species, even though with some spread. The maximum peak values reached ~23,000 (H₂O),
15
16
17 208 ~20,000 (CO₂), 118 (H₂S), 62 (SO₂) and 30 (H₂) ppmv.

19 209 The molar compositions of fumarolic gases from the 17 individualized vents (Tab. 1) confirm
20
21 210 this spatial heterogeneity. Each fumarole actually exhibited stable, well-resolved composition (see
22
23
24 211 the fumarole 15 example in Figure 3). Instead, the SO₂/H₂S ratios in all fumaroles span more than
25
26 212 three orders of magnitude, from 0.001 to 1.5 (Tab. 1 and Fig. 3). The H₂O/H₂S, CO₂/H₂S, and
27
28 213 H₂/H₂S also varied considerably within the fumarolic field, with respective ranges of 98-480, 108-
29
30
31 214 240 and 0.05-0.24 (Tab. 1 and Fig. 3).

33 215 Table 2 shows the chemistry of dry gases collected from the hottest (315°C) F15 fumarole (Fig.
34
35 216 2d, e). CO₂ is the overwhelming component (up to 97%), followed by H₂S (around 1%), H₂ (952-
36
37 217 979 ppm), CO (15-17 ppm) and CH₄ (around 1-2 ppm). N₂ and O₂ contents reflect air
38
39 218 contamination of the samples, with minimum values of 0.5% and 0.1%. The concentration of
40
41
42 219 helium is around 8 ppm in our less contaminated sample. Whatever the degree of air contamination,
43
44 220 our samples from the hottest F15 fumarole reveal CO₂/H₂S (94-107) and H₂/H₂S (0.09-0.10) ratios
45
46
47 221 (Tab. 2) that are very comparable to the corresponding ratios determined with Multi-GAS.

49 222 The SO₂/H₂S ratio is a commonly used marker to distinguish the magmatic (SO₂-rich) vs.
50
51 223 hydrothermal (H₂S-rich) nature of volcanic gas (e.g. AIUPPA *et alii*, 2005b). Figure 4 shows that
52
53
54 224 Pico do Fogo fumaroles define a nearly continuous trend from two end-members:

56 225 (i) a magmatic end-member, represented by the hottest gas from fumaroles 14-15 (T = 315-316
57
58 226 °C), characterized by H₂O/CO₂ of ~ 2, CO₂/S_t of ~ 100, high SO₂ (~0.2 mol. %) and
59
60

1
2
3 227 relatively low H₂S, and oxidised (redox conditions of about 1 log unit above the Nickel-
4
5 228 Nickel Oxide buffer at ~500°C, estimated from the measured SO₂/H₂S ~ 0.9-1.4 and
6
7
8 229 H₂/H₂O ~ 0.0004; see methodology in AIUPPA et al., 2011); and,

9
10 230 (ii) a hydrothermal end-member, represented by fumaroles 3-8, that is H₂S-dominated (~0.35-
11
12 231 0.43 mol. %; SO₂/H₂S of ~ 0.01-0.2), relatively richer in CO₂ (CO₂/S_t > 130 and
13
14
15 232 H₂O/CO₂ < 1) and more reduced (H₂/H₂O > 0.0015) (corresponding to redox conditions
16
17 233 close to the FeO-FeO1.5 buffer; GIGGENBACH, 1987).
18

19 234 The red star in Figures 4a-d represents the spatially integrated composition of Pico do Fogo's
20
21 235 fumarolic emission, calculated as the arithmetic mean of compositions of the 17 main fumaroles. It
22
23
24 236 is characterized by the following ratios, normalized to H₂S: SO₂/H₂S = 0.3±0.4, H₂O/H₂S =
25
26 237 299±109, CO₂/H₂S = 153±33 and H₂/H₂S = 0.2±0.04 (Tab. 1). The mean SO₂/H₂S ratio of ~0.3 is
27
28
29 238 not much different from the SO₂/H₂S ratio of 0.12 of the bulk volcanic plume (Tab. 1 and Fig. 4)
30
31 239 determined after 30-min continuous Multi-GAS measurements made on the outer crater rim (see
32
33 240 "bulk plume Multi-GAS site" in Fig. 2b, e). At that Multi-GAS site, we could intercept only a very
34
35 241 dilute plume, rising buoyantly from the fumarolic field inside the crater floor (Fig. 2d). Only small
36
37
38 242 concentrations of H₂S (~ 1 ppmv) and SO₂ (~ 0.15 ppmv) could be detected, no volcanic H₂O, CO₂,
39
40 243 or H₂ being resolvable from the air background. Given these very low H₂S and SO₂ concentrations,
41
42 244 well below our calibration range (10-200 ppmv), the inferred bulk plume SO₂/H₂S ratio of 0.12
43
44
45 245 must be considered with caution; we just take it as indication that hydrothermal H₂S-rich fumaroles
46
47 246 prevail over the more magmatic end-member fumaroles in the bulk gas emission from Pico do
48
49 247 Fogo, in agreement with indications from the arithmetic mean of fumarolic compositions.
50

51 248 52 53 54 249 SO₂ FLUX

55
56 250 Figure 5a presents the SO₂ flux time-series obtained by the UV Camera on February 5, 2019. A
57
58 251 plot of SO₂ column amounts along the UV cross-section of Fig. 5b shows that, thanks to the short
59
60

1
2
3 252 distance (~200 m) between the camera and the targeted plume, a feeble but continuous SO₂
4
5 253 emission (<400 ppm·m; mean, 140±110 ppm·m) was detected by the UV Camera in the leftmost
6
7
8 254 portion of the camera FoV (Fig. 5c), and persisted throughout the ~100 minutes of recording (Fig.
9
10 255 5a). During our measurement interval the SO₂ flux varied between 0.3 and 2.3 tons/day (or 0.009 to
11
12 256 0.06 kg/s) and averaged at 1.4±0.4 tons/day (0.016±0.004 kg/s).

13
14
15 257
16
17 258
18
19 259
20
21
22 260

23 24 261 **DISCUSSION**

25 26 262 THE COMPOSITION OF PICO DO FOGO FUMARoles

27
28 263 The molar gas ratios determined by Multi-GAS measurements allow us to compute the molar
29
30
31 264 percentages of H₂O, CO₂, H₂S, SO₂ and H₂ in each fumarole and in the mean gas composition
32
33 265 (Table 1). These percentages for only the 5 above species are upper bounds since we did not
34
35 266 determine other possible minor species (N₂, HCl) in the gases. Otherwise, they are not affected by
36
37
38 267 the presence of reduced carbon species, whose amount was verified to be very low in F5 fumarole
39
40 268 this study and (MELIÁN *et alii*, 2015). According to our results, the Pico do Fogo fumaroles are
41
42 269 moderately hydrous (41-73 % H₂O; mean, 64 %), CO₂-rich (27-59 %; mean, 36 %), and contain
43
44
45 270 about ~0.3 % S_t and 0.04 % H₂ (Tab. 1). These mean values match well the composition of the F15
46
47 271 fumarole, directly sampled and analysed in laboratory, as regards the H₂/H₂S and CO₂/H₂S molar
48
49 272 ratios (Tab. 2).

50
51 273 The triangular plot in Figure 6 puts the H₂O-CO₂-S_t compositions of our Pico do Fogo fumaroles
52
53
54 274 in a wider context, by comparing them against the compositions of (i) the 2014 Fogo eruption
55
56 275 plume (HERNÁNDEZ *et alii*, 2015), which represents the only available datum for the Fogo
57
58 276 magmatic gas signature to date; (ii) magmatic gases from other intraplate, rift and/or divergent-plate
59
60

1
2
3 277 volcanoes (see AIUPPA, 2015 for data sources); and (iii) fumaroles from other volcanic systems in
4
5 278 the Macaronesia region, including the Azores (CALIRO *et alii*, 2005; FERREIRA & OSKARSSON,
6
7 279 1999; FERREIRA *et alii*, 2005; MARES project, this study) and Teide in the Canary (MELIÁN *et alii*,
8
9 280 2012; MARES project, this study).

11
12 281 The Pico do Fogo summit fumaroles (this study) are compositionally distinct from the magmatic
13
14 282 gases released during the 2014 eruption (HERNÁNDEZ *et alii*, 2015), this latter falling well within
15
16 283 the range of measured magmatic gas compositions at other intraplate volcanoes (yellow field, from
17
18 284 AIUPPA, 2015). More specifically, the summit Fogo fumaroles are evidently S-depleted relative to
19
20 285 the 2014 magmatic gas, which strongly suggests intense sub-surface scrubbing of reactive S
21
22 286 compounds under the “hydrothermal” conditions of the fumarolic field, where surface temperatures
23
24 287 (≤ 315 °C) are well below the boiling temperature of liquid sulfur (455 °C; above which S
25
26 288 scrubbing become minimal, if any; AIUPPA *et alii*, 2017). Extensive S deposition in the sub-surface
27
28 289 environment of the summit fumaroles is further supported by CO_2/S_t ratios being far higher in the
29
30 290 fumaroles (93-162) than in the 2014 eruption gas (1.5; HERNÁNDEZ *et alii*, 2015) (Figs. 6, 7). The
31
32 291 two hottest summit fumaroles (F14 and F15) consistently display the lowest CO_2/S_t ratios (93-97),
33
34 292 but these are still two orders of magnitude higher than in the eruptive gas, confirming the
35
36 293 importance of sulfur scrubbing (Fig. 7). This is also verified for the dry gases directly sampled from
37
38 294 fumarole F15, whose $\text{CO}_2/\text{H}_2\text{S}$ ratio is 94-107 (Tab. 2).

39
40 295 Fogo summit fumaroles are also less hydrous (or more CO_2 -rich) than the 2014 eruptive gas
41
42 296 (Fig. 6). If the 2014 gas is representative of the magmatic gas feeding the summit fumaroles (a
43
44 297 magmatic gas supply is indeed supported by the low but measurable SO_2 output; Fig. 5), then the
45
46 298 simplest explanation of H_2O depletion in the fumaroles is extensive steam condensation in the
47
48 299 fumarolic conduits due to low temperature conditions. Because our Multi-GAS measurements were
49
50 300 made in air-diluted (and cooled) fumarolic plumes, we cannot entirely exclude that partial H_2O
51
52 301 condensation could have also occurred during plume transport and/or in the Multi-GAS inlet system
53
54
55
56
57
58
59
60

1
2
3 302 (tubing + filter), such as previously observed at other volcano-hydrothermal systems (e.g., ALLARD
4
5 303 *et alii*, 2014; LOPEZ *et alii*, 2017; TAMBURELLO *et alii*, 2019). However, we note that our Multi-
6
7
8 304 GAS-derived H₂O range (41-73 %) partially overlaps with the H₂O range (52-92 %) for the summit
9
10 305 Fogo fumaroles previously determined from direct gas sampling (MELIÁN *et alii*, 2015). We thus
11
12 306 conclude that both subsurface and within-plume H₂O condensation may combine to drive the
13
14 307 summit fumaroles toward a less hydrous and correspondingly CO₂-enriched composition compared
15
16
17 308 to the 2014 eruptive gas. We cannot exclude, however, that the magmatic gas that feeds the
18
19 309 persistent summit fumaroles is compositionally different from the 2014 eruptive gas. If for example
20
21 310 the magmatic gas source is the Pico do Fogo magma reservoir located in the uppermost mantle at
22
23 311 16–28 km depth (HILDNER *et alii*, 2011, 2012; MATA *et alii*, 2017), then it is well possible that
24
25
26 312 its composition has deeper (CO₂-richer, H₂O-S-poorer) signature than that of eruptive 2014 gas
27
28
29 313 (derived from shallow degassing).

30
31 314 The Pico do Fogo fumaroles plot at the CO₂-rich end of the compositional array defined by
32
33 315 volcanic hydrothermal fluids in the Macaronesian region (Fig. 6). The majority of volcanic
34
35 316 fumaroles from the Azores (Sao Miguel, Terceira and Graciosa islands) and from Teide volcano in
36
37 317 the Canaries are shifted toward the H₂O corner. This is a typical (but not exclusive) feature of most
38
39
40 318 hydrothermal steam vents worldwide (CHIODINI & MARINI, 1998), which reflects their derivation
41
42 319 from the boiling of meteoric groundwater-fed hydrothermal systems (CALIRO *et alii*, 2015). The
43
44 320 less hydrous compositions of Pico do Fogo fumaroles suggest the absence of a shallow boiling
45
46
47 321 hydrothermal aquifer underneath Pico's summit, and consequently a weaker (relative to Azores and
48
49 322 Teide) hydrothermal fingerprint (greater magmatic signature), especially in the hottest fumaroles
50
51 323 (F14 and F15) that also exhibit lower CO₂/S_t ratios (Fig. 7) and higher SO₂/H₂S ratios (Fig. 4).
52
53 324 These SO₂-bearing F14-F15 fluids appear as formerly magmatic gases that have undergone partial
54
55
56 325 H₂O-S_t loss (via condensation + scrubbing) during cooling and hydrothermal re-equilibration (Fig.
57
58 326 6). Instead, the most SO₂-poor, H₂S-dominated fumaroles (e.g., F3-F8) have suffered more
59
60

1
2
3 327 significant hydrothermal processing, as testified by their lower H_2O/CO_2 (< 1), higher CO_2/S_t ($>$
4
5 328 130), and more reduced (H_2 -rich) redox conditions, typical of hydrothermal fluids (FISCHER &
6
7
8 329 CHIODINI, 2015) (Figs. 4, 7).

9
10 330 To conclude, we attribute the CO_2 -rich compositions of the Pico do Fogo fumaroles to a
11
12 331 combination of (i) hydrothermal interactions (partially removing magmatic sulphur and water) and
13
14
15 332 possibly (ii) a deep magmatic gas source.

16 17 333 18 19 334 GAS OUTPUT BUDGET

20
21 335 Combining the compositional data described above with the UV camera-based SO_2 flux record
22
23
24 336 depicted in Figure 5, we can reliably estimate the output of CO_2 and other volatiles from the summit
25
26 337 crater fumarolic field of Pico do Fogo (Table 3). To do this calculation, we combine the measured
27
28
29 338 mean SO_2 flux (1.4 ± 0.4 tons/day) and the mean molar composition of the summit fumaroles
30
31 339 (64.1 ± 9.2 % H_2O , 35.6 ± 9.1 % CO_2 , 0.2 ± 0.08 % H_2S , 0.06 ± 0.06 % SO_2 , and 0.04 ± 0.02 % H_2 ; red
32
33 340 star in Figs. 4, 6 and 7), the S_t (0.26 ± 0.14 %) of which is scaled to the bulk plume SO_2/H_2S ratio of
34
35 341 0.12 (Tab. 1 and Fig. 4) to infer the bulk plume mass ratios at 558 (H_2O/SO_2), 756 (CO_2/SO_2), 4.2
36
37
38 342 (H_2S/SO_2) and 1.1 (H_2/SO_2), respectively. This procedure allows us to smooth the effect of the large
39
40 343 compositional heterogeneity of the fumarolic vents. We just note that the bulk plume SO_2/H_2S ratio
41
42 344 of 0.12 characterizes the predominance of H_2S -dominated (F3-F8-like) hydrothermal fluids over
43
44
45 345 more SO_2 -rich (F14-F15-like) “more magmatic” fumaroles.

46
47 346 We obtain a daily fumarolic CO_2 output of 1060 ± 340 tons (Table 3). We also estimate a daily
48
49 347 release of 780 ± 320 H_2O , 6.2 ± 2.4 H_2S and 0.05 ± 0.022 H_2 . These results demonstrate that the
50
51
52 348 fumarolic gas output is larger, for all volatiles, than diffuse degassing through the crater floor
53
54 349 (DIONIS *et alii*, 2014, 2015) (Fig. 8). For example, the latter has been estimated to produce 147-219
55
56 350 (± 35) tons/day of CO_2 (DIONIS *et alii*, 2014, 2015), which is only 14-20% of the inferred fumarolic
57
58 351 CO_2 output. Even considering the soil CO_2 output estimated at the scale of the entire island (828 ± 5
59
60

1
2
3 352 tons/day; DIONIS *et alii*, 2015), the contribution of diffuse degassing remains less than a half (~
4
5 353 43%) of the total Fogo island CO₂ degassing budget (~1890 tons/day; this study and DIONIS *et alii*,
6
7
8 354 2015).

9
10 355 In contrast, the daily fumarolic gas output is far lower than the eruptive gas output (Fig. 8) for
11
12 356 the 2014 eruption derived by HERNÁNDEZ *et alii*, (2015) by combining SO₂ flux measurements with
13
14
15 357 a scanning UV spectrometer (using the Differential Optical Absorption Spectroscopy – DOAS -
16
17 358 technique) and a Multi-GAS-derived plume composition. Our fumarolic SO₂ output, for example, is
18
19 359 a factor ~7000 lower than the large (~10 ktons) daily eruptive release (HERNÁNDEZ *et alii*, 2015).
20
21 360 Let emphasize, however, that while summit fumarolic emissions at Fogo have persisted as a stable
22
23
24 361 degassing feature over the past few centuries (RIBEIRO, 1960), eruptive degassing has been
25
26 362 restricted to the relatively infrequent eruptions. There are only 10 reported eruptions since 1785
27
28
29 363 (RIBEIRO, 1960), of which only 3 since 1951 (HILDNER *et alii*, 2011, 2012; CARRACEDO *et alii*,
30
31 364 2015; MATA *et alii*, 2017). Between June 12, 1951 (the onset of the first, well recorded XX century
32
33 365 eruption; HILDNER *et alii*, 2012) and February 8, 2015 (the end of the last eruption), Fogo has been
34
35 366 in eruption for only 200 days (e.g., 0.008 % of the 24710 elapsed days). If we take the November
36
37
38 367 30, 2015 gas output (HERNÁNDEZ *et alii*, 2015) as typical for Fogo eruptive daily degassing rate, we
39
40 368 can roughly compute a cumulative eruptive release for 1951-2015 (200 days of eruption) of ~4
41
42 369 Mtons of H₂O, ~2 Mtons of CO₂ and SO₂, 11 ktons of H₂S and 0.04 ktons of H₂. These masses,
43
44
45 370 when scaled to (integrated over) the 24710 days elapsed from June 12, 1951 to February 8, 2015,
46
47 371 correspond to daily eruptive outputs of only 196, 86, 82, 0.5 and 0.002 tons/day for H₂O, CO₂, SO₂,
48
49 372 H₂S and H₂, respectively (Fig. 8). Our back-of-the-envelope calculations demonstrate that, when
50
51
52 373 examined on longer-term perspective, eruptive emissions at Fogo are significant for only SO₂, while
53
54 374 they do make a relatively small contribution to the emission budget of other volatiles (Fig. 8).

55
56 375 We therefore conclude that summit crater fumarolic emissions at Pico do Fogo are the dominant
57
58 376 source of volcanic CO₂ (and most other volatiles) over multi-decadal scale.

60

378 IMPLICATIONS FOR THE GLOBAL CO₂ OUTPUT INVENTORY

379 On a broader perspective, our results for Pico do Fogo in Cape Verde archipelago add a new
380 piece of information to the global catalogue of volcanic CO₂ emissions. Recent work (FISCHER *et*
381 *alii*, 2019; WERNER *et alii*, 2019) has attempted at refining the global volcanic CO₂ emission
382 inventory, by reviewing, cataloguing and synthesizing the volcanic CO₂ output information
383 available in the international literature. It was found that, by late 2019, CO₂ flux measurements have
384 become available for 102 of the ~500 degassing subaerial volcanoes worldwide (FISCHER *et alii*,
385 2019; WERNER *et alii*, 2019; FISCHER & AIUPPA, 2020 submitted). Different strategies have been
386 used to extrapolate the cumulative CO₂ output “measured” for the 102 volcanoes (~44 Tg/yr) to
387 CO₂ emissions from the several hundred “unmeasured” subaerial degassing volcanoes. These have
388 included the use of independent rock-chemistry information (AIUPPA *et alii*, 2019) and/or the
389 identification of statistical properties (mean CO₂ output and confidence intervals) for different
390 categories of volcanoes. On the latter basis, it was proposed that the present-day global volcanic
391 CO₂ budget is dominated by the category of Strong Volcanic Gas Emitters (S_{vge}) – which includes
392 the ~100 top degassing volcanoes whose SO₂ emissions are systematically detected from space-
393 borne and/or ground-based spectrometers (CARN *et alii*, 2017; FISCHER *et alii*, 2019). S_{vge} have an
394 inferred total (extrapolated) CO₂ output of ~ 36-39 Tg/yr (AIUPPA *et alii*, 2019; FISCHER *et alii*,
395 2019). It was additionally found that a group of Weak Volcanic Gas Emitters (W_{vge}), although
396 degassing in a more subtle manner (this category includes volcanoes with no visible plumes and/or
397 minor to absent SO₂ emissions), may still contribute between 15 (FISCHER *et alii*, 2019) and 35
398 (WERNER *et alii*, 2019) Tg CO₂/yr, simply because they are numerous (~400) globally.
399 Unfortunately, however, these results are subject to very large uncertainties because measuring the
400 CO₂ output from quiescent/hydrothermal volcanoes is especially challenging from a technical

1
2
3 401 viewpoint (indirect SO₂ flux-based estimates are hampered by low to absent SO₂; WERNER *et alii*,
4
5 402 2019), making the CO₂ flux catalogue particularly incomplete for W_{vge}.

7
8 403 Pico do Fogo falls within the W_{vge} category, as no plume is visually observable (Fig. 2) and no
9
10 404 SO₂ is detectable by satellite except during the infrequent eruptions (GLOBAL VOLCANISM
11
12 405 PROGRAM, 2017). Our results show, however, that SO₂ is present in tiny but measurable quantities
13
14 406 in the fumaroles (Table 1), making both the SO₂ flux and, indirectly, the CO₂ flux (Table 3)
15
16
17 407 measurable from a very proximal location on ground (Fig. 2; note that a test made with UV-Camera
18
19 408 from the base of the volcano were unable to detect any SO₂ release).

21
22 409 When put in the context of global volcanic CO₂ fluxes (Fig. 9; data from FISCHER *et alii*, 2019),
23
24 410 the fumarolic CO₂ flux from Pico do Fogo (ca. 1000 tons/day) confirms that W_{vge} volcanoes can
25
26 411 emit CO₂ in quantities that, in some cases, can rival the emissions of S_{vge} volcanoes. High CO₂
27
28 412 emission from such W_{vge} systems, despite negligible (hydrothermal-dominant) to weak (magmatic-
29
30
31 413 hydrothermal) SO₂ emission (FISCHER *et alii*, 2019), result from their exceptionally high CO₂/S_t
32
33 414 signature (AIUPPA *et alii*, 2017). Pico do Fogo fumaroles are not an exception, but owing to their
34
35 415 high CO₂/S_t compositions they can sustain a CO₂ output of order 1000 tons/day, at the upper range
36
37
38 416 of the global W_{vge} and S_{vge} populations (Fig. 9). Therefore, our present results further demonstrate
39
40 417 that refining the global inventory for volcanic CO₂ output will require enhanced quantification of
41
42 418 the weaker, poorly visible emissions sustained by quiescent hydrothermal volcanoes, the majority of
43
44
45 419 which still lack CO₂ flux quantification.

46 47 420 CONCLUSIONS

49 421 We have shown here that fumarolic activity on-top of Pico do Fogo volcano, in the Atlantic Cape
50
51 422 Verde archipelago, is currently a poorly visible but substantial source of volcanic volatiles to the
52
53
54 423 atmosphere. The fumarolic CO₂ output (~1060 tons/day), in particular, is found to exceed by far the
55
56 424 time-integrated eruptive CO₂ flux (~86 tons/day) from the volcano, as well as the estimated total
57
58 425 CO₂ budget from soil degassing across Fogo island (147-828 tons/day). On a broader scale, our
59
60

1
2
3 426 results confirm that quiescent volcanoes characterized by hydrothermal activity during quiescent
4
5 427 stages can produce CO₂ emissions that rival those of more manifestly degassing (Strong Volcanic
6
7
8 428 Gas Emitters, S_{vge}) owing to their CO₂-enriched fumarole compositions (CO₂/S_t ratios of 93-163 at
9
10 429 Pico do Fogo in 2019). At Pico do Fogo, these CO₂-enriched compositions likely result from the
11
12 430 interactions (scrubbing of magmatic sulphur, and water condensation) of a deep magmatic gas
13
14 431 supply (perhaps sourced from a 16–28 km deep magma reservoir in the uppermost mantle; HILDNER
15
16
17 432 *et alii*, 2011, 2012; MATA *et alii*, 2017) with a shallow hydrothermal system.
18

19 433 20 21 434 ACKNOWLEDGEMENTS

22
23
24 435 This research was funded by the Portuguese Fundação para a Ciência e a Tecnologia (MARES
25
26 436 project - PTDC/GEO-FIQ/1088/2014), the DECADE project of the Deep Carbon Observatory, and
27
28 437 the Italian Ministero Istruzione Università e Ricerca (Grant n. 2017LMNLAW). We thank
29
30 438 Francesco Salerno and Manfredi Longo from INGV-Palermo for providing support with gas
31
32
33 439 chromatographic analysis. The manuscript benefited from constructive reviews from Taryn Lopez,
34
35 440 Yuri Taran and from the Associate Editor Orlando Vaselli.
36
37
38 441

39 40 442 REFERENCES

- 41
42 443 AIUPPA A. (2015) - *Volcanic-gas monitoring* In: *Volcanism and Global Environmental Change*, pp.
43
44 444 81-96. Cambridge University Press. doi: 10.1007/9781107415683.007.
45
46
47 445 AIUPPA A., FEDERICO C., GIUDICE G. & GURRIERI S. (2005a) - *Chemical mapping of a fumarolic*
48
49 446 *field: La Fossa Crater, Vulcano Island (Aeolian Islands, Italy)*. Geophysical Research Letters,
50
51 447 **32**, 4.
52
53
54 448 AIUPPA A., INGUAGGIATO S., MCGONIGLE A.J.S., O'DWYER M., OPPENHEIMER C., PADGETT M.J.,
55
56 449 ROUWET D. & VALENZA M. (2005b) - *H₂S fluxes from Mt. Etna, Stromboli, and Vulcano (Italy)*
57
58
59
60

- 1
2
3 450 *and implications for the sulfur budget at volcanoes. Geochim. Cosmochim. Acta, 69 (7), 1861-*
4
5
6 451 1871.
- 7
8 452 AIUPPA A., SHINOHARA H., TAMBURELLO G., GIUDICE G., LIUZZO M., MORETTI R., (2011) –
9
10 453 *Hydrogen in the gas plume of an open-vent volcano, Mount Etna, Italy. J. Geophys. Res. B:*
11
12 454 *Solid Earth 116 (10), B10204.*
- 14
15 455 AIUPPA A. ET ALII (2015) - *New ground-based lidar enables volcanic CO₂ flux measurements. Sci.*
16
17 456 *Reports 5, 13614.*
- 19 457 AIUPPA A., LO COCO E., LIUZZO M., GIUDICE G., GIUFFRIDA G. & MORETTI R. (2016) - *Terminal*
20
21 458 *Strombolian activity at Etna's central craters during summer 2012: The most CO₂-rich volcanic*
22
23 459 *gas ever recorded at Mount Etna. Geochemical Journal, 50 (2), 123-138.*
- 26 460 AIUPPA A., FISCHER T.P., PLANK T., ROBIDOUX P. & DI NAPOLI R. (2017) - *Along-arc, interarc and*
27
28 461 *arc-to-arc variations in volcanic gas CO₂/S_T ratios reveal dual source of carbon in arc*
29
30 462 *volcanism. Earth Science Reviews 168, 24–47.*
- 33 463 AIUPPA A., FISCHER T.P., PLANK T. & BANI P. (2019) - *CO₂ flux emissions from the Earth's most*
34
35 464 *actively degassing volcanoes, 2005–2015. Sci. Reports 9:5442, [https://doi.org/10.1038/s41598-](https://doi.org/10.1038/s41598-019-41901-y)*
36
37 465 *[019-41901-y](https://doi.org/10.1038/s41598-019-41901-y).*
- 40 466 ALLARD P., AIUPPA A., BEAUDICEL, GAUDIN D., DI NAPOLI R., CRISPI O., CALABRESE S., PARELLO
41
42 467 F., HAMMOUYA G., TAMBURELLO G. (2014) *Steam and gas emission rate from La Soufriere*
43
44 468 *volcano, Guadeloupe (Lesser Antilles): implications for the magmatic supply during degassing*
45
46 469 *unrest. Chemical Geology 384, 76–93*
- 49 470 ASIMOW P.D., DIXON J.E. & LANGMUIR C.H. (2004) - *A hydrous melting and fractionation model*
50
51 471 *for mid-ocean ridge basalts: application to the Mid-Atlantic Ridge near the Azores.*
52
53 472 *Geochemistry, Geophysics, Geosystems 5, doi:10.1029/2003GC000568.*
- 56 473 BONATTI E. (1990) - *Not so hot 'hot spots' in the oceanic mantle. Science 250, 107-111.*
57
58
59
60

1

2

3 474 BRUNE S., WILLIAMS S.E. & MÜLLER R.D. (2017) - *Potential links between continental rifting, CO₂*
4
5 475 *degassing and climate change through time*. Nat. Geosci., **10**, 941–946. doi: 10.1038/s41561-
6
7 476 017-0003-6.

9

10 477 CALIRO S., VIVEIROS F., CHIODINI G. & FERREIRA T. (2015) - *Gas geochemistry of hydrothermal*
11
12 478 *fluids of the S. Miguel and Terceira Islands, Azores*. Geochimica et Cosmochimica Acta, **168**,
13
14 479 43-57. doi: 10.1016/j.gca.2015.07.009.

16

17 480 CAPPELLO A., GANCI G., CALVARI S., PÉREZ N.M., HERNÁNDEZ P.A., SILVA S.V., CABRAL J. & DEL
18
19 481 NEGRO C. (2016) - *Lava flow hazard modeling during the 2014-2015 Fogo eruption, Cape*
20
21 482 *Verde*. Journal of Geophysical Research: Solid Earth, **121** (4), pp. 2290-2303.

23

24 483 CARN S.A., FIOLETOV V.E., MCLINDEN C.A., LI C. & KROTKOV N.A. (2017) - *A decade of global*
25
26 484 *volcanic SO₂ emissions measured from space*. Sci. Reports 7:44095, doi: 10.1038/srep44095.

27

28 485 CARRACEDO J.-C., PEREZ-TORRADO F.J., RODRIGUEZ-GONZALEZ A., PARIS R., TROLL V.R. &
29
30 486 BARKER A.K. (2015) - *Volcanic and structural evolution of Pico do Fogo, Cape Verde*. Geology
31
32 487 Today, **31** (4), pp. 146-152.

34

35 488 CHIODINI G. & MARINI L. (1998) - *Hydrothermal gas equilibria: The H₂O-H₂-CO₂-CO-CH₄ system*.
36
37 489 Geochim. Cosmochim. Acta, **62** (15), 2673-2687. doi: 10.1016/S0016-7037(98)00181-1.

39

40 490 CHRISTENSEN B., HOLM P., JAMBON A. & WILSON J. (2001) - *Helium, argon and lead isotopic*
41
42 491 *composition of volcanics from Santo Antão and Fogo, Cape Verde Islands*. Chemical Geology,
43
44 492 **178**, 127–142.

46

47 493 COURTNEY R.C. & WHITE R.S. (1986) - *Anomalous heat-flow and geoid across the Cape- Verde*
48
49 494 *rise — evidence for dynamic support from a thermal plume in the mantle*. Geophysical Journal
50
51 495 International, **87** (3), 815–867.

53

54 496 CROUGH S.T. (1978) - *Thermal origin of mid-plate hot-spot swells*. Geophys. J. R. Astron. Soc., **55**,
55
56 497 451– 469.

57

58

59

60

- 1
2
3 498 CROUGH S.T. (1982) - *Geoid anomalies over the Cape Verde Rise*. Mar. Geophys. Res., **5**, 263–
4
5 499 271, doi:10.1007/BF00305564.
6
7
8 500 DASGUPTA R. (2013). *Ingassing, storage, and outgassing of terrestrial carbon through geologic*
9
10 501 *time*. Rev. Mineral. Geochem., **75**, 183–229. doi: 10.2138/rmg.2013.75.7.
11
12 502 DASGUPTA R. & HIRSCHMANN M.M. (2010) - *The deep carbon cycle and melting in Earth's*
13
14 503 *interior*. Earth Planet. Sci. Lett., **298**, 1–13. doi: 10.1016/j.epsl.2010.06.039.
15
16
17 504 DAVIES G.F., NORRY M.J., GERLACH D.C. & CLIFF R.A. (1989) - *A combined chemical and Pb-Sr-*
18
19 505 *Nd isotope study of the Azores and Cape Verde hotspots: The geodynamic implications, in*
20
21 506 *Magmatism in the Ocean Basins*. In Saunders A.D. & Norry M.J. Geol. Soc. Spec. Publ.,
22
23 507 **42**,231–255.
24
25
26 508 Day, S.J., Heleno Da Silva, S.I.N., Fonseca, J.F.B.D. A past giant lateral collapse and present-day
27
28 509 flank instability of Fogo, Cape Verde Islands (1999) Journal of Volcanology and Geothermal
29
30 510 Research, 94 (1-4), pp. 191-218.
31
32
33 511 Day, S.J., Carracedo, J., Guillou, H., Pais Pais, F., Rodriguez Badiola, E., Fonseca, J., Heleno da
34
35 512 Silva, S., 2000. Comparison and cross-checking of historical, archaeological and geological
36
37 513 evidence for the location and type of historical and sub-historical eruptions of multiple-vent
38
39 514 oceanic island volcanoes. In: McGuire, W., Griffiths, D., Hancock, P., Stewart, I. (Eds.), The
40
41 515 Archaeology of Geological Catastrophes: Geological Society, London, Special Publications,
42
43 516 London, pp. 281–306.
44
45
46 517 DELLE DONNE D., AIUPPA A., BITETTO M., D'ALEO R., COLTELLI M., COPPOLA D., PECORA E.,
47
48 518 RIPEPE M. & TAMBURELLO G. (2019) - *Changes in SO₂ Flux regime at Mt. Etna captured by*
49
50 519 *automatically processed ultraviolet camera data*. Remote Sensing, **11** (10), art. no. 1201.
51
52
53 520 DIONIS S.M., MELIÁN G., RODRÍGUEZ F., HERNÁNDEZ P.A., PADRÓN E., PÉREZ N.M., BARRANCOS J.,
54
55 521 PADILLA G., SUMINO H., FERNANDES P., BANDOMO Z., SILVA S., PEREIRA J.M. & SEMEDO H.
56
57
58
59
60

1
2
3
4
5
6
7
8
9
10
11
12
13
14
15
16
17
18
19
20
21
22
23
24
25
26
27
28
29
30
31
32
33
34
35
36
37
38
39
40
41
42
43
44
45
46
47
48
49
50
51
52
53
54
55
56
57
58
59
60

- 522 (2014) - *Diffuse volcanic gas emission and thermal energy release from the summit crater of*
523 *Pico do Fogo, Cape Verde*. *Bulletin of Volcanology*, **77** (2), 13 p.
- 524 DIONIS S.M., PÉREZ N.M., HERNÁNDEZ P.A., MELIÁN G., RODRÍGUEZ F., PADRÓN E., SUMINO H.,
525 BARRRANCOS J., PADILLA G.D., FERNANDES P., BANDOMO Z., SILVA S., PEREIRA J.M., SEMEDO,
526 H. & CABRAL J. (2015) - *Diffuse CO₂ degassing and volcanic activity at Cape Verde Islands,*
527 *West Africa*. *Earth, Planets and Space*, **67** (1), art. no. 48.
- 528 Doucelance R., Escrig S., Moreira M., Gariépy C. & Kurz M.D. (2003) - *Pb-Sr-He isotope and*
529 *trace element geochemistry of the Cape Verde Archipelago*. *Geochim. Cosmochim. Acta*, **67**,
530 3717–3733.
- 531 FERREIRA T. & OSKARSSON N. (1999) - *Chemistry and isotopic composition of fumarole discharges*
532 *of Furnas caldera*. *J. Volcanol. Geotherm. Res.* **92**, 169–179.
- 533 FERREIRA T., GASPAR J.L., VIVEIROS F., MARCOS M., FARIA C. & SOUSA F. (2005) - *Monitoring of*
534 *fumarole discharge and CO₂ soil degassing in the Azores: contribution to volcanic surveillance*
535 *and public health risk assessment*. *Ann. Geophys.* **48**, 787–796.
- 536 FISCHER T.P. (2013) - *DEep CARbon DEgassing: The Deep Carbon Observatory DECADE*
537 *Initiative*. *Mineralogical Magazine*, **77**(5), 1089.
- 538 FISCHER T.P. & AIUPPA A. (2020). *Global CO₂ emissions from subaerial volcanism: recent*
539 *progresses and future challenges*. *Geochem. Geophys., Geosyst.*, under consideration.
- 540 FISCHER T.P. & CHIODINI G. (2015). *Volcanic, Magmatic and Hydrothermal Gases*. In: *The*
541 *Encyclopedia of Volcanoes*, 2nd Edition, Edited by H. Sigurdsson, B. Houghton, S. McNutt, H.
542 Rymer, J. Stix Elsevier, doi: 10.1016/B978-0-12-385938-9.00045-6
- 543 FISCHER T.P., ET ALII (2019) - *The emissions of CO₂ and other volatiles from the world's subaerial*
544 *volcanoes*. *Sci. Rep.*, **9**:18716, <https://doi.org/10.1038/s41598-019-54682-1>.

- 1
2
3 545 GERLACH D.C., CLIFF C.A., DAVIES G.R., NORRY M.J. & HODGSON N. (1988) - *Magma sources of*
4
5 546 *the Cape Verdes archipelago: Isotopic and trace element constraints*. *Geochim. Cosmochim.*
6
7 547 *Acta*, **52**, 2979–2992. doi:10.1016/0016-7037(88)90162-7.
9
10 548 GERLACH T.M. (1991) - *Present-day carbon dioxide emissions from volcanoes*. *Earth in Space* 4, 5.
11
12 549 Global Volcanism Program, 2017. Report on Fogo (Cape Verde). In: Crafford A.E. & Venzke E.
13
14 (eds.), *Bulletin of the Global Volcanism Network*, **42**, 9. Smithsonian Institution.
15 550 <https://doi.org/10.5479/si.GVP.BGVN201709-384010>.
16
17 551
18
19 552 GIGGENBACH W.F. (1987), *Redox processes governing the chemistry of fumarolic gas discharges*
20
21 553 *from White Island, New Zealand*, *Appl. Geochem.*, **2**, 143–161, doi:10.1016/0883-
22
23 554 2927(87)90030-8.
24
25
26 555 HERNÁNDEZ P.A. (2015) - *Chemical composition of volcanic gases emitted during the 2014-15*
27
28 556 *Fogo eruption, Cape Verde*. *Geophysical Research Abstracts*, Vol. **17**, EGU2015-9577, 2015,
29
30 EGU General Assembly 2015.
31 557
32
33 558 HILDNER E., KLÜGEL A. & HAUFF F. (2011) - *Magma storage and ascent during the 1995 eruption*
34
35 559 *of Fogo, Cape Verde Archipelago*. *Contributions to Mineralogy and Petrology*, **162 (4)**, 751.
36
37 560 doi:10.1007/s00410-011-0623-6.
38
39
40 561 HILDNER H., KLÜGEL A. & HANSTEEN T. (2012) - *Barometry of lavas from 1951 eruption of Fogo,*
41
42 562 *Cape Verde Islands: implications for historic and prehistoric magma plumbing system*. *Journal*
43
44 563 *of Volcanology and Geothermal Research*, **217-218**, 73–90.
45
46
47 564 HOERNLE K., TILTON G., LE BAS M.J., DUGGEN S. & GARBE-SCHÖNBERG D. (2002) - *Geochemistry*
48
49 565 *of oceanic carbonatites compared with continental carbonatites: mantle recycling of oceanic*
50
51 566 *crustal carbonate*. *Contributions to Mineralogy and Petrology*, **142(5)**, 520-542.
52
53
54 567 HOLM P.M., WILSON J.R., CHRISTENSEN B.P., HANSEN L., HANSEN S.L., HEIN K.M., MORTENSEN
55
56 568 A.K., PEDERSEN R., PLESNER S. & RUNGE M.K. (2006) - *Sampling the Cape Verde mantle plume:*
57
58
59
60

1
2
3
4
5
6
7
8
9
10
11
12
13
14
15
16
17
18
19
20
21
22
23
24
25
26
27
28
29
30
31
32
33
34
35
36
37
38
39
40
41
42
43
44
45
46
47
48
49
50
51
52
53
54
55
56
57
58
59
60

- 569 *evolution of the melt compositions on Santo Antão, Cape Verde Islands*. *Journal of Petrology*, **47**,
- 570 145–189.
- 571 HOLM P.M., GRANDVUINET T., FRIIS J., WILSON J.R., BARKER A.K. & PLESNER S. (2008) - *An ⁴⁰Ar–*
- 572 *³⁹Ar study of the Cape Verde hot spot: temporal evolution in a semistationary plate environment*.
- 573 *Journal of Geophysical Research* **113 (B8)**, B08201.
- 574 KANTZAS E.P., MCGONIGLE A.J.S., TAMBURELLO G., AIUPPA A. & BRYANT R.G. (2010) - *Protocols*
- 575 *for UV camera volcanic SO₂ measurements*. *J. Volcanol. Geotherm. Res.*, **194**, 55–60.
- 576 KERN C., KICK F., LÜBCKE P., VOGEL L., WÖHRBACH M. & AND PLATT U. (2010) - *Theoretical*
- 577 *description of functionality, applications, and limitations of SO₂ cameras for the remote sensing*
- 578 *of volcanic plumes*. *Atmos. Meas. Tech.*, **3**, 733–749, www.atmos-meas-tech.net/3/733/2010/
- 579 doi:10.5194/amt-3-733-2010.
- 580 KOGARKO L.N., RYABUKHIN V.A. & VOLYNETS M.P. (1992), *Cape Verde Island carbonatite*
- 581 *geochemistry*. *Geochem. Int.*, **29**, 62–74.
- 582 ILYINSKAYA E, AIUPPA A, BERGSSON B ET ALII (2015) - *Degassing regime of Hekla volcano 2012–*
- 583 *2013*. *Geochim. Cosmochim. Acta*, **159**. 80-99.
- 584 ILYINSKAYA E., MOBBS S., BURTON R., BURTON M., PARDINI F., PFEFFER M.A., ET ALII (2018) -
- 585 *Globally significant CO₂ emissions from Katla, a Subglacial Volcano in Iceland*. *Geophys. Res.*
- 586 *Lett.*, **45**, 332–310. doi: 10.1029/2018GL079096.
- 587 LIU X. & ZHAO D. (2014) - *Seismic evidence for a mantle plume beneath the Cape Verde hotspot*.
- 588 *International Geology Review*, **56**, 1213–1225.
- 589 LOPEZ T., ET ALII, (2017) - *Geochemical constraints on volatile sources and subsurface conditions*
- 590 *at Mount Martin, Mount Mageik, and Trident Volcanoes, Katmai*. *J. Volcanol. Geotherm. Res.*,
- 591 **347** 64–81, <https://doi.org/10.1016/j.jvolgeores.2017.09.001>.

- 1
2
3 592 MARQUES F.O., CATALÃO J.C., DEMETS C., COSTA A.C.G. & HILDENBRAND A. (2013) - *GPS and*
4
5 593 *tectonic evidence for a diffuse plate boundary at the Azores Triple Junction*. Earth and Planetary
6
7 594 Science Letters **381**, 177-187.
9
- 10 595 MARQUES F.O., HILDENBRAND A., VICTÓRIA S.S., CUNHA D. & DIAS, P. (2020) - *Caldera or flank*
11
12 596 *collapse in the Fogo volcano? What age? Consequences for risk assessment in volcanic islands*.
13
14 597 Journal of Volcanology and Geothermal Research (in press),
16
17 598 <https://doi.org/10.1016/j.jvolgeores.2019.106686>
18
- 19 599 MATA J., MOREIRA M., DOUCELANCE R., ADER M. & SILVA, L.C. (2010) - *Noble gas and carbon*
20
21 600 *isotopic signatures of Cape Verde oceanic carbonatites: implications for carbon provenance*.
22
23 601 Earth and planetary Science Letters, **291**, 70–83.
25
- 26 602 MATA J., MARTINS S., MATTIELLI N., MADEIRA J., FARIA B., RAMALHO R.S., SILVA P., MOREIRA M.,
27
28 603 CALDEIRA R., RODRIGUES J. & MARTINS L. (2017) - *The 2014–15 eruption and the short-term*
29
30 604 *geochemical evolution of the Fogo volcano (Cape Verde): Evidence for small-scale mantle*
31
32 605 *heterogeneity*. Lithos, **288–289**, 91–107.
34
- 35 606 MELIÁN G., TASSI F., PÉREZ N., HERNÁNDEZ P., SORTINO F., VASELLI O., PADRÓN E., NOLASCO D.,
36
37 607 BARRANCOS J., PADILLA G., RODRÍGUEZ F., DIONIS S., CALVO D., NOTSU K. & SUMINO H. (2012)
38
39 608 - *A magmatic source for fumaroles and diffuse degassing from the summit crater of Teide*
40
41 609 *Volcano (Tenerife, Canary Islands): A geochemical evidence for the 2004-2005 seismic-volcanic*
42
43 610 *crisis*. Bulletin of Volcanology, **74 (6)**, 1465-1483.
45
- 46 611 MELIÁN G.V., ET ALII (2015) - *Insights from fumarole gas geochemistry on the recent volcanic*
47
48 612 *unrest of Pico do Fogo, Cape Verde*. Geophysical Research Abstracts, Vol. **17**, EGU2015-
49
50 613 12754, 2015, EGU General Assembly 2015.
52
- 53 614 MÉTRICH N., ZANON V., CRÉON L., HILDENBRAND A., MOREIRA M., MARQUES F.O. (2014) - *Is the*
54
55 615 *“Azores hotspot” a wet spot? Insights from geochemistry of fluid and melt inclusions in olivines*
56
57 616 *of Pico basalts*. J. Petrol. **55**, 377-393
59
60

1
2
3
4
5
6
7
8
9
10
11
12
13
14
15
16
17
18
19
20
21
22
23
24
25
26
27
28
29
30
31
32
33
34
35
36
37
38
39
40
41
42
43
44
45
46
47
48
49
50
51
52
53
54
55
56
57
58
59
60

- 617 MILLET M.A., DOUCELANCE R., SCHIANO P., DAVID K. & BOSQ C. (2008) - *Mantle plume*
618 *heterogeneity versus shallow-level interactions: a case study, the São Nicolau Island, Cape*
619 *Verde archipelago*. Journal of Volcanology and Geothermal Research, **176(2)**, 265-276.
- 620 MONTELLI R., NOLET G., DAHLEN F.A. & MASTERS G. (2006) - *A catalogue of deep mantle plumes:*
621 *new results from finite-frequency tomography*. Geochemistry, Geophysics, Geosystems **7**,
622 <http://dx.doi.org/10.1029/2006GC001248>
- 623 MOURÃO, C., MOREIRA, M., MATA, J., RAQUIN, A., MADEIRA, J (2012) *Primary and secondary*
624 *processes constraining the noble gas isotopic signatures of carbonatites and silicate rocks from*
625 *Brava Island: evidence for a lower mantle origin of the Cape Verde plume*. Contributions to
626 Mineralogy and Petrology **163**, 995–1009.
- 627 PEDONE M. ET ALII (2014) - *Volcanic CO₂ flux measurement at Campi Flegrei by tunable diode*
628 *laser absorption spectroscopy*. Bulletin of Volcanology, **76**, 13.
- 629 QUEIBER M., GRANIERI D. & BURTON M. (2016) - *A new frontier in CO₂ flux measurements using a*
630 *highly portable DIAL laser system*. Scientific Reports, **6**, 33834.
- 631 RIBEIRO O. (1960) - *A Ilha do Fogo e as suas erupções (The island of Fogo and its eruptions)*. 2nd
632 edn. Memórias, serie geographica I. Junta de Investigações do Ultramar. Ministerio do Ultramar,
633 Lisbon.
- 634 RICHTER N., FAVALLI M., DE ZEEUW-VAN DALFSEN E., FORNACIAI A., DA SILVA FERNANDES R.M.,
635 PÉREZ N.M., LEVY J., VICTÓRIA S.S. & WALTER T.R. (2016) - *Lava flow hazard at Fogo*
636 *Volcano, Cabo Verde, before and after the 2014-2015 eruption*. Natural Hazards and Earth
637 System Sciences, **16 (8)**, pp. 1925-1951.
- 638 Saki, M., Thomas, C., Nippress, S.E.J., Lessing, S., 2015. Topography of upper mantle seismic
639 discontinuities beneath the North Atlantic: the Azores, Canary and Cape Verde plumes. Earth
640 and Planetary Science Letters **409**, 193–202

- 1
2
3 641 TAMBURELLO G. (2015) - *Ratiocalc: Software for processing data from multicomponent volcanic*
4
5 642 *gas analyzers*. *Comput. Geosci.*, **82**, 63–67.
- 7
8 643 TAMBURELLO G., KANTZAS E.P., MCGONIGLE A.J.S. & AIUPPA A. (2011) - *Vulcamera, a program*
9
10 644 *for measuring volcanic SO₂ using UV cameras*. *Ann. Geophys.* **54**, 2.
- 12
13 645 TAMBURELLO G., AIUPPA A., KANTZAS E.P., MCGONIGLE A.J.S. & RIPEPE M. (2012) - *Passive vs.*
14
15 646 *active degassing modes at an open-vent volcano (Stromboli, Italy)*. *Earth Planet. Sci. Lett.*, **359–**
16
17 647 **360**, 106–116.
- 19
20 648 TAMBURELLO G., MOUNE S., ALLARD P., VENUGOPAL S., ROBERT V., ROSAS-CARNAJAL M.,
21
22 649 UCCIANI G., DEROUSSI S, KITOU T., DIDIER T., KOMOROWSKI J-C., BEAUDICEL F., DE CHABALIER
23
24 650 J-B., LEMARCAHND A., MORETTI R., DESSERT C. (2019) *Spatio-temporal relationships between*
25
26 651 *fumarolic activity, hydrothermal fluid circulation and geophysical signals at an arc volcano in*
27
28 652 *degassing unrest: La Soufrière of Guadeloupe (French West Indies)*. *Geosciences*, **9**, 480-507
29
30 653 doi:10.3390/geosciences9110480.
- 32
33 654 TARAN, Y., KALACHEVA, E. (2019) - *Role of hydrothermal flux in the volatile budget of a*
34
35 655 *subduction zone: Kuril arc, northwest Pacific*. *Geology*, 47 (1), 87-90. doi: 10.1130/G45559.1
- 37
38 656 TARAN, Y.A. (2009) - *Geochemistry of volcanic and hydrothermal fluids and volatile budget of the*
39
40 657 *Kamchatka-Kuril subduction zone* *Geochimica et Cosmochimica Acta*, 73 (4), 1067-1094. , doi:
41
42 658 10.1016/j.gca.2008.11.020
- 44
45 659 VAN DER MEER D.G., ZEEBE R.E., VAN HINSBERGEN D.J.J., SLUIJS A., SPAKMAN W. & TORSVIK T.H.
46
47 660 (2014) - *Plate tectonic controls on atmospheric CO₂ levels since the Triassic*. *Proc. Natl. Acad.*
48
49 661 *Sci. U.S.A.* 111, 4380–4385. doi:10.1073/pnas.1315657111.
- 51
52 662 WERNER C., EVANS W. C., POLAND M., TUCKER D.S. & DOUKAS M.P. (2009) - *Long-term changes*
53
54 663 *in quiescent degassing at Mount Baker Volcano, Washington, USA; evidence for a stalled*
55
56 664 *intrusion in 1975 and connection to a deep magma source*. *Journal of Volcanology and*
57
58 665 *Geothermal Research* **186**, 379–386.
- 59
60

1
2
3 666 WERNER C., ET ALII, (2019) - *Carbon Dioxide Emissions from Subaerial Volcanic Regions: Two*
4
5 667 *Decades in Review*. In: Orcutt B.N, Daniel I. & Dasgupta R. *Deep Carbon, Past to Present*.
6
7 Cambridge University Press www.cambridge.org/9781108477499, doi:
8 668
9 10.1017/9781108677950.
10 669
11

12 670 WONG K, MASON E., BRUNE S, EAST M., EDMONDS M. & ZAHIROVIC S. (2019) - *Deep Carbon*
13
14 *Cycling Over the Past 200 Million Years: A Review of Fluxes in Different Tectonic Settings*.
15 671
16 Front. Earth Sci. **7**, 263. doi: 10.3389/feart.2019.00263.
17 672
18

19 673
20

21 674 **FIGURE CAPTIONS**

22
23
24 675 **Figure 1** - Google Earth image (Image © 2019 Maxar Technologies) of (a) the Cape Verde
25
26 676 archipelago and (b) Fogo Island.

27
28
29 677 **Figure 2** – (a) Panoramic view of Pico do Fogo volcano; (b) Map of the Pico do Fogo summit
30
31 678 crater, showing (i) a thermal map of the fumarolic field; (ii) the position of the 17 analysed
32
33 679 fumaroles (red circles, see (e) for a detail; white numbers identify fumaroles 1, 8 and 17 for
34
35 680 reference); (iii) the UV Camera measurement site (FOV and “cross section” are the Field of View
36
37 681 of the camera and the ICA integration section, respectively); and (iv) the Bulk-plume Multi-Gas
38
39 682 measurement site. The base map is from Bing Maps (<https://www.bing.com/maps>, Microsoft Ltd);
40
41
42 683 (c) the inner crater seen from the Bulk-plume Multi-Gas measurement site; (d) the fumarolic field
43
44 684 seen from the UV Camera measurement site. The plume transport direction is indicated by white
45
46 685 arrows. The position of some selected fumaroles (red circles with identification numbers) are shown
47
48 686 for reference; (e) A zoom of the inner crater (base map as in (a)), showing the track of the Multi-
49
50 687 GAS walking traverse and the positions of the 17 fumaroles (red circles with white labels; see Tab 1
51
52 688 for GPS positions). All measurements were performed on February 5, 2019.
53
54

55
56 689 **Figure 3** – Scatter plots of H₂O, CO₂, SO₂ and H₂ concentrations vs H₂S in the plumes of
57
58 690 summit crater fumaroles at Pico do Fogo. Open circles stand for the 4446 concentration
59
60

1
2
3 691 measurements performed during the ~74-minute-long Multi-GAS walking traverse. H₂O, CO₂ and
4
5 692 H₂ concentrations are corrected for air background (see text). In each plot, solid lines and grey-
6
7 filled area identify the range (minimum, maximum) of X/H₂S gas ratios in the identified 17
8 693 individual fumaroles (see Table 1). The large spread of compositions, indicated by the large ratio
9
10 694 interval (especially for the SO₂/H₂S ratio, varying from 0.001 to 1.5), attests to the chemical
11
12 695 heterogeneity of the fumarolic field. Otherwise, each of the 17 fumaroles exhibited stable, well-
13
14 696 resolved X/H₂S ratios, as here illustrated by the F15 fumarole example (grey-filled circles).

15
16
17 697
18
19 698 **Figure 4** – Scatter plots of SO₂/H₂S ratios in the 17 fumaroles vs. (a) H₂O/H₂S ratios, (b)
20
21 699 H₂O/CO₂ ratios, (c) CO₂/S_t ratios, and (d) H₂/H₂O ratios (data from Table 1). The SO₂/H₂S ratio is
22
23 taken as a good indicator of the magmatic (high-SO₂) vs. hydrothermal (high-H₂S) signature of each
24 700 fumarole. The measured fumaroles define a nearly continuous trend between a “magmatic” gas end-
25
26 701 member, represented by the SO₂-richer, hydrous (H₂O/CO₂ ~ 2) and more oxidised (low H₂/H₂O)
27
28 702 F14-F15 fumaroles, and a hydrothermal (H₂S-dominated) end-member (exemplified by fumaroles
29
30 F3-F8), richer in CO₂ (CO₂/S_t > 130 and H₂O/CO₂ < 1) and more reduced (H₂/H₂O > 0.0015). Note
31 703 that we directly collected 3 dry-gas samples of fumarole F15 for comparison, which yield a CO₂/S_t
32
33 704 ratio range of 94-107 (Table 2; pink horizontal bar labelled “DS” in (c)) nearly identical to the
34
35 705 Multi-GAS-derived ratio (97; Table 1). In each plot the red star identifies the average (arithmetic
36
37 706 mean of the 17 fumaroles) composition of the fumarolic field (Table 1), while the vertical grey bar
38
39 (“BULK”) indicates the SO₂/H₂S ratio measured in the bulk plume from the outer rim (site in Fig.
40 707 2).
41
42 708
43
44 709
45
46
47 710
48

49 711 **Figure 5** – (a) SO₂ flux time-series obtained with the UV Camera from the “UV Camera”
50
51 712 measuring site indicated in Figure 2. Blue diamonds are individual data (obtained every 2 seconds)
52
53 while the red line is for a 60 sec mobile average; (b) a pseudo-colour image obtained by
54 713 combination of two simultaneously taken (by the two co-exposed UV cameras) images, showing the
55
56 714 inner crater wall, and the ICA integration section (UV cross-section); (c) an example of SO₂ column
57
58 715
59
60

1
2
3
4
5
6
7
8
9
10
11
12
13
14
15
16
17
18
19
20
21
22
23
24
25
26
27
28
29
30
31
32
33
34
35
36
37
38
39
40
41
42
43
44
45
46
47
48
49
50
51
52
53
54
55
56
57
58
59
60

716 amount (in ppm·m) variation along the camera pixels over the UV cross-section shown in (b). The
717 plume is identified by higher-than-background SO₂ column amounts (0-400 ppm·m) between
718 camera pixels 0 and ~200.

Figure 6 – H₂O/10-CO₂-5S_t triangular plot comparing the compositions of Pico do Fogo summit fumaroles (yellow circles, data from Table 1; red star mean composition as in Figure 4) with the compositions of (i) the 2014-2015 Fogo eruptive plume (orange circle labelled “FO”; HERNÁNDEZ *et alii*, 2015) (ii) hydrothermal vents from the Macaronesia (see legend) and worldwide (crosses; CHIODINI & MARINI, 1998). Also shown for comparison are the compositional fields of arc magmatic gases and intraplate/rift magmatic gases (AIUPPA, 2015). The white circles identify compositions for some intraplate /rift volcanoes (HE: Hekla; ER: Erebus; NY: Nyiragongo; KI: Kilauea summit; KE: Kilauea east rift zone; AR: Ardoukoba; PDF: Piton de la Fournaise; EA: Erta Ale; SU: Surtsey; see AIUPPA, 2015 for data provenance). Grey lines identify some characteristic CO₂/S_t and H₂O/CO₂ ratios (see grey numbers on axes). The effects of S scrubbing, H₂O condensation or addition are illustrated by the red lines (with arrows).

Figure 7 – (a) Temperature dependence of CO₂/S_t (molar) ratios in the Macaronesia fumarolic gas samples. At Pico do Fogo, we measured temperatures (with a thermocouple) in only the three hottest vents (F5, F14 and F15). The CO₂/S_t (molar) ratios in hydrothermal fluids from volcanoes in the Azores and from Teide (Tenerife, Canary) are shown for comparison in both (a) and in the zoom of (b). The latter shows that CO₂/S_t ratios in fumaroles from Azores-Canary are negatively correlated with temperature, as observed globally (AIUPPA *et alii*, 2017). For reference, we also show in both panels the CO₂/S_t ratio signature of Fogo magmatic gas, as determined by Multi-GAS plume measurements during the 2014-2015 eruption (HERNÁNDEZ *et alii*, 2015; see also Figure 6).

Figure 8 – Volatile outputs from different types of gas emissions on Fogo island: (i) the summit fumarolic field, this study; (ii) diffuse soil degassing from the crater area and the whole island

1
2
3
4
5
6
7
8
9
10
11
12
13
14
15
16
17
18
19
20
21
22
23
24
25
26
27
28
29
30
31
32
33
34
35
36
37
38
39
40
41
42
43
44
45
46
47
48
49
50
51
52
53
54
55
56
57
58
59
60

740 (DIONIS *et alii*, 2014, 2015); and (iii) eruptive degassing (HERNÁNDEZ *et alii*, 2015 and recalculated;
741 see text for explanation).

Figure 9 – Histogram showing the logarithmic distribution of the population of measured/predicted CO₂ fluxes (in tons/day) from subaerial volcanoes. Data are from Fischer *et alii*, (2019) except for Pico do Fogo (this study). Following FISCHER *et alii*, (2019) and FISCHER & AIUPPA (2019, submitted), volcanoes are distinguished in two sub-categories: 1) Strong Volcanic Gas Emitters (S_{vge}, in red), including the 125 top degassing volcanoes whose SO₂ emissions have systematically been detected from space-borne and/or ground-based spectrometers (CARN *et alii*, 2017; FISCHER *et alii*, 2019); and 2) Weak Volcanic Gas Emitters (W_{vge}), including volcanoes with no visible plumes and weak SO₂ emissions. Like in FISCHER *et alii*, (2019) and FISCHER & AIUPPA, (2020, submitted), W_{vge} are further divided into hydrothermal volcanoes, with minor to absent (< 8 tons/day) SO₂ emissions (yellow), and magmatic-hydrothermal volcanoes with somewhat higher (> 8 tons/day, but still undetectable from space) SO₂ emissions (orange). Pico do Fogo, although falling in the subcategory of W_{vge} (SO₂ < 8 tons/day) emits CO₂ at the upper W_{vge} range, and at levels comparable to (or higher than) many S_{vge}.

Table 1 – Results of Multi-GAS observations on Pico do Fogo fumarolic field on February 5, 2019. We report composition obtained for 17 fumaroles, the atmospheric plumes of which were measured for a few minutes each (time start – time end is GMT time). Temperature was measured in three fumaroles only using a portable thermocouple. For each fumarole, we report the peak SO₂ concentration (SO₂ max) measured during the acquisition interval and the volatile ratios (normalised to H₂S) calculated with Ratiocalc (Tamburello, 2015) using the scatter-plot technique. For each ratio, mean is the slope of the best-fit regression line and R² is the corresponding correlation coefficient. We also report the recalculated molar percentages (mol. %) in the fumaroles and some representative molar ratios. *Mean fumarole composition (and 1 standard deviation, 1 SD) calculated by averaging the compositions of the 17 fumaroles. The bulk plume was measured for its SO₂/H₂S ratio only from the crater rim site shown in Figure 2. †Ratios determined on the same F15 fumarole using direct sampling (data from Tab. 2).

Fumarole ID	T	LAT	LONG	Time Start	Time End	SO ₂ max	Mean	R ²	Error	Mean	R ²	Error	Mean	R ²	Error	Mean	R ²	Error	mol%	mol%	mol%	mol%	mol%	molar	molar	molar	molar	
	°C					ppm	SO ₂ /H ₂ S	SO ₂ /H ₂ S	SO ₂ /H ₂ S	CO ₂ /H ₂ S	CO ₂ /H ₂ S	CO ₂ /H ₂ S	H ₂ /H ₂ S	H ₂ /H ₂ S	H ₂ /H ₂ S	H ₂ O/H ₂ S	H ₂ O/H ₂ S	H ₂ O/H ₂ S	H ₂ O	CO ₂	H ₂ S	SO ₂	H ₂	H ₂ O/CO ₂	H ₂ O/S _{tot}	CO ₂ /S _t	H ₂ /H ₂ O	
1		14.95046	-24.34111	13:27	13:30	3.9	0.15	0.85	0.04	149	0.99	10	0.18	0.884	0.04	318	0.97	39	67.9	31.8	0.21	0.03	0.04	2.1	276	130	0.00057	
2		14.95063	-24.34071	13:31	13:32	4.9	0.16	0.65	0.12	136	0.96	30	0.13	0.848	0.06	260	0.97	49	65.5	34.2	0.25	0.04	0.03	1.9	224	117	0.00050	
3		14.95069	-24.34072	13:32	13:33	0.6	0.001	0.53	0.01	135	0.99	37	0.165	0.99	0.03	98	0.94	55	41.7	57.8	0.43	0.00	0.07	0.7	98	135	0.00169	
4		14.9507	-24.34072	13:33	13:36	3.8	0.05	0.53	0.03	117	0.94	20	0.13	0.677	0.06	184	0.90	59	61.0	38.6	0.33	0.02	0.04	1.6	175	111	0.00071	
5	225	14.95067	-24.3408	13:36	13:40	8.8	0.14	0.65	0.06	133	0.99	8	0.15	0.91	0.03	284	0.96	33	68.0	31.7	0.24	0.03	0.04	2.1	249	116	0.00053	
6		14.95066	-24.34072	13:41	13:46	5.2	0.36	0.90	0.22	134	0.99	7	0.18	0.918	0.03	277	0.96	27	67.2	32.4	0.24	0.09	0.04	2.1	203	98	0.00065	
7		14.95045	-24.34072	13:46	13:48	4.3	0.15	0.96	0.03	131	1.00	7	0.11	0.886	0.03	236	0.93	57	64.2	35.5	0.27	0.04	0.03	1.8	205	114	0.00047	
8		14.95032	-24.34078	13:49	13:51	5.1	0.03	0.78	0.01	167	0.99	12	0.24	0.949	0.04	116	0.61	80	40.8	58.7	0.35	0.01	0.08	0.7	113	163	0.00206	
9		14.95044	-24.34065	13:52	13:55	6.9	0.05	0.64	0.02	108	0.99	7	0.14	0.932	0.02	192	0.82	54	63.7	35.9	0.33	0.02	0.05	1.8	183	103	0.00073	
10		14.95061	-24.34068	13:57	14:00	35.2	0.79	0.85	0.21	207	0.98	18	0.15	0.82	0.04	404	0.92	74	65.9	33.7	0.16	0.13	0.02	2.0	226	115	0.00037	
11		14.95066	-24.34072	14:00	14:04	6.5	0.23	0.82	0.06	149	0.98	12	0.13	0.885	0.03	374	0.96	44	71.4	28.3	0.19	0.04	0.02	2.5	304	121	0.00035	
12		14.95067	-24.34085	14:04	14:11	1.4	0.2	0.86	0.03	176	0.98	9	0.16	0.395	0.08	356	0.87	56	66.7	33.1	0.19	0.04	0.03	2.0	296	147	0.00045	
13		14.95073	-24.34088	14:11	14:15	5.8	0.22	0.91	0.04	148	0.99	8	0.15	0.84	0.04	390	0.94	57	72.3	27.4	0.19	0.04	0.03	2.6	319	121	0.00038	
14	316	14.95064	-24.34064	14:17	14:18	24.7	0.85	0.33	1.42	172	0.70	134	0.05	0.144	0.14	311	0.62	283	64.1	35.5	0.21	0.18	0.01	1.8	168	93	0.00016	
15	315	14.95064	-24.34065	14:18	14:20	61.5	1.48	0.71	0.88	240	0.95	54	0.2	0.884	0.07 (0.09-0.1)†	482	0.97	73	66.5	33.2	0.14	0.20	0.03	2.0	194	97 (94-107)†	0.00042	
16		14.95062	-24.34061	14:21	14:25	14.2	0.45	0.83	0.11	160	0.98	13	0.14	0.916	0.02	442	0.89	81	73.2	26.6	0.17	0.07	0.02	2.8	305	111	0.00032	
17		14.95071	-24.34055	14:26	14:32	9.1	0.28	0.89	0.04	154	0.99	7	0.17	0.915	0.02	362	0.92	44	69.9	29.8	0.19	0.05	0.03	2.3	283	120	0.00047	
MEAN*							0.3			153			0.2			299			64.1	35.6	0.2	0.06	0.04	1.9	225	118	0.00064	
1 SD*							0.4			33			0.04			109			9.2	9.1	0.08	0.06	0.02	0.6	67	18	0.00049	
BULK		14.95073	-24.34196	11:37	12:01	0.15	0.12	0.70	0.04	-	-	-	-	-	-	-	-	-	-	-	-	-	-	-	-	-	-	-

Table 2 - Chemistry (in mol %) of major and minor dry gas components in Pico do Fogo F15 fumarole. H₂/H₂S and CO₂/H₂S ratios are reported for comparison with the same ratios calculated by Multi-GAS

Sample	T °C	date	He ppm	H ₂ ppm	O ₂ %	N ₂ %	CH ₄ ppm	CO ppm	CO ₂ %	H ₂ S %	Tot %	H ₂ /H ₂ S	CO ₂ /H ₂ S
F15a	315	05/02/2019	8	952	0.11	0.51	0.7	15	97.03	1.03	98.8	0.09	94.20
F15b			8	979	0.33	1.4	1.3	17	95.83	0.96	98.6	0.10	99.82
F15c			6	373	12.63	46.35	2.1	13	39.6	0.37	99.0	0.10	107.03

Table 3 - Volatile fluxes from Fogo island. All data in tons/day

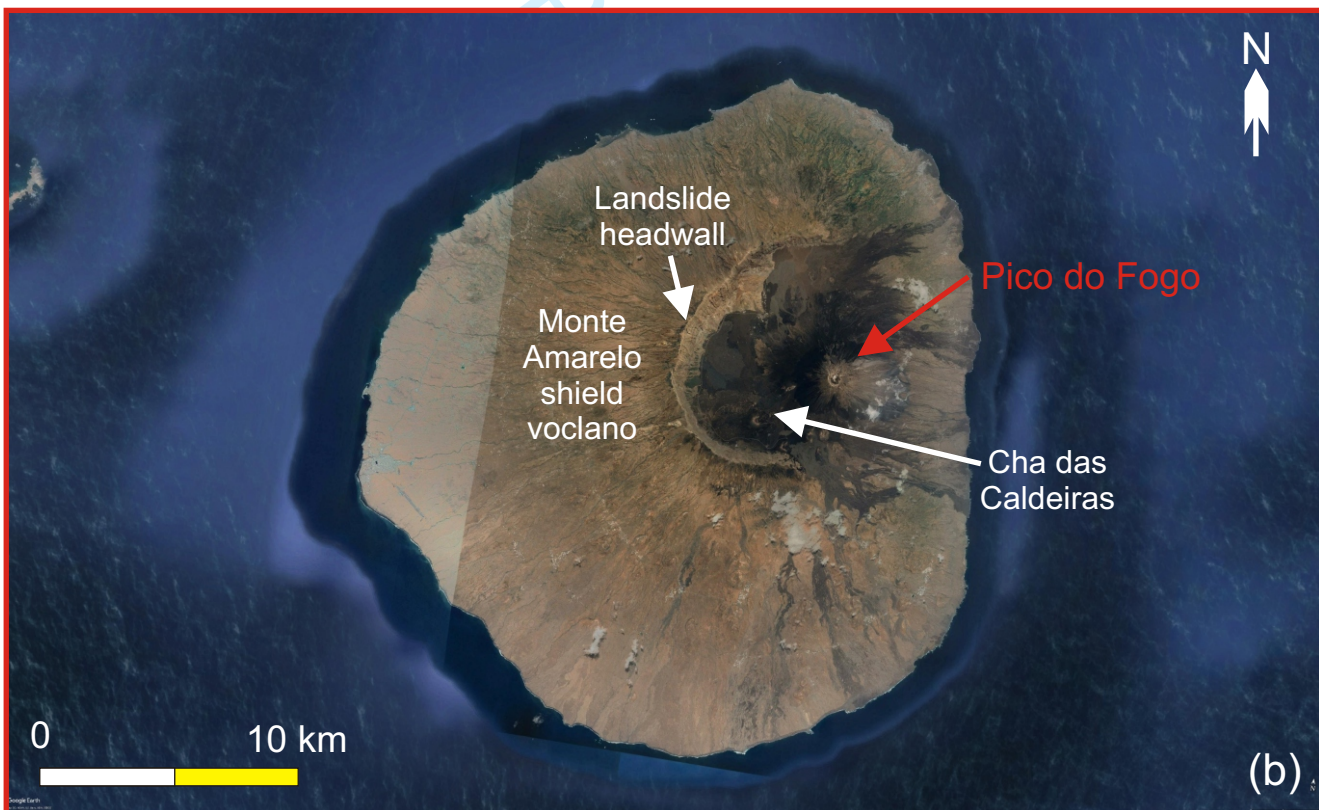
	Summit Fumarolic Field*		Diffuse Degassing ^o		Eruptive degassing (2014 eruption) [£]	Eruptive degassing (time integrated) [§]
	Mean	1 SD	Mean	1 SD	Mean	Mean
SO₂ flux	1.4	0.4	-	-	10118	82
H₂O flux	780	320	330	-	24245	196
CO₂ flux	1060	340	147-219 (828@)	35-36	10668	86
H₂S flux	6.2	2.4	0.025	0.007	57	0.5
H₂ flux	0.05	0.022	0.033	0.0105	0.2	0.002

*This work; ^oinner crater floor; Dionis et al., 2014; @whole island; Dionis et al., 2015; [£]Measured on November 30, 2014; Hernández et al., 2015; [§]This study, recalculated from data in Hernández et al., 2015

1
2
3
4
5
6
7
8
9
10
11
12
13
14
15
16
17
18
19
20
21
22
23
24
25
26
27
28
29
30
31
32
33
34
35
36
37
38
39
40
41
42
43
44
45
46
47
48
49
50
51
52
53
54
55
56
57
58
59
60

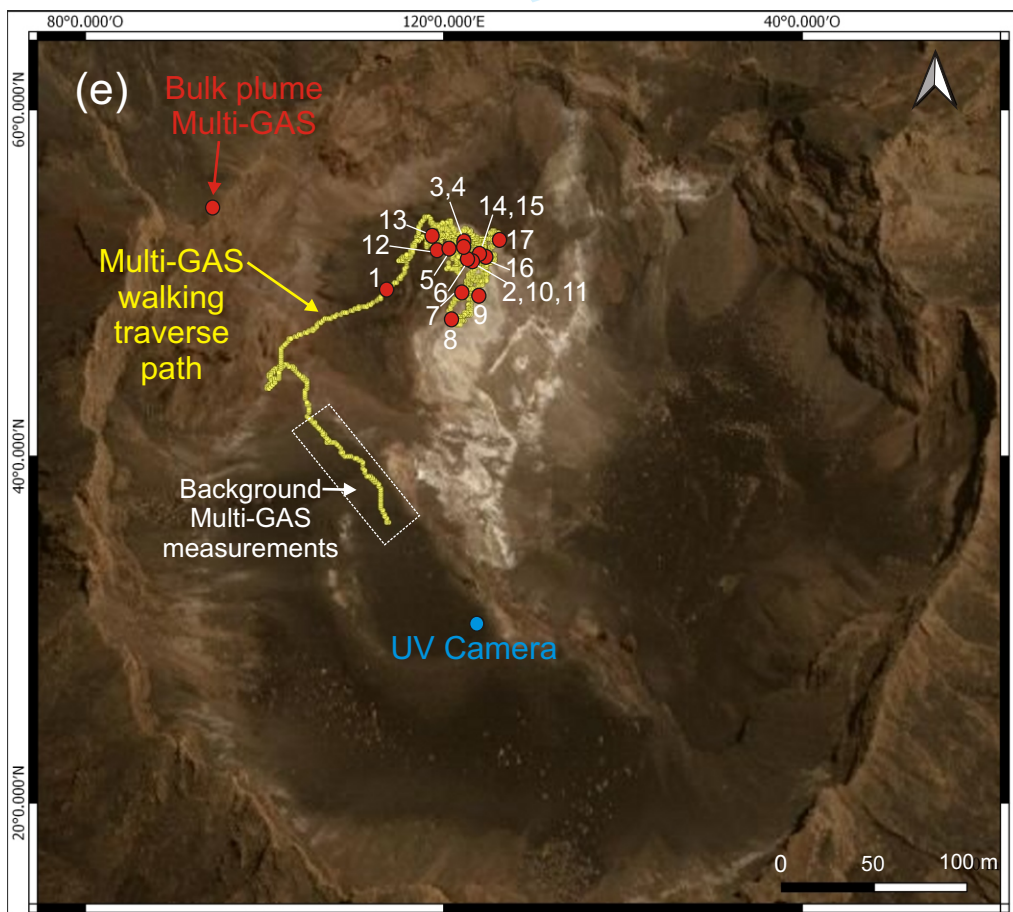
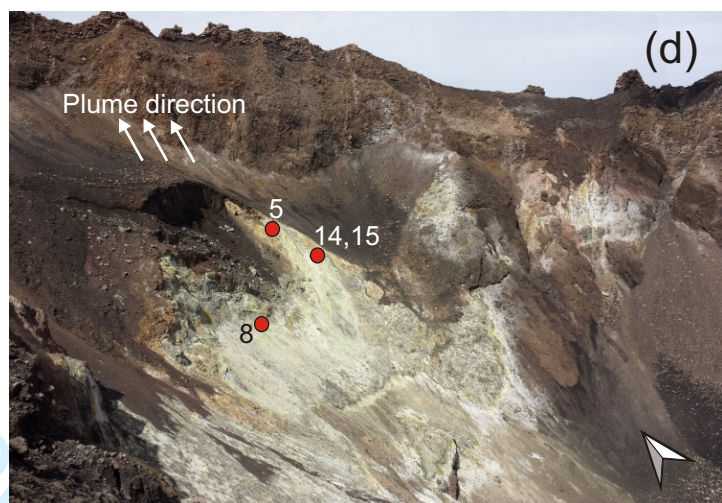
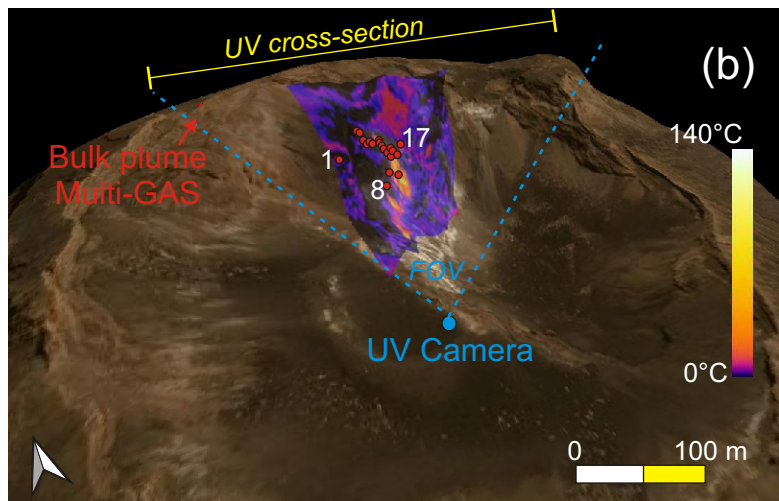


14°40'24"N

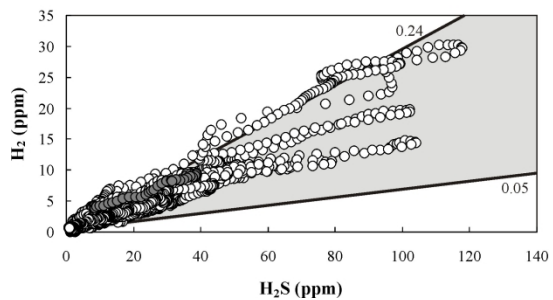
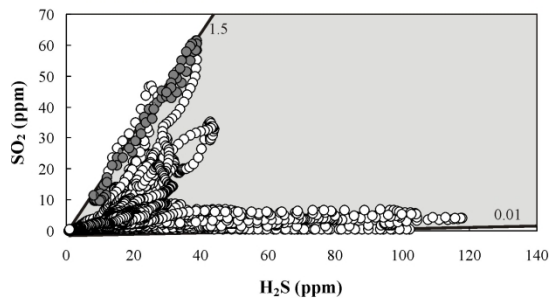
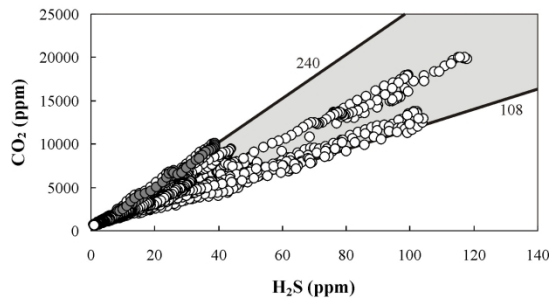
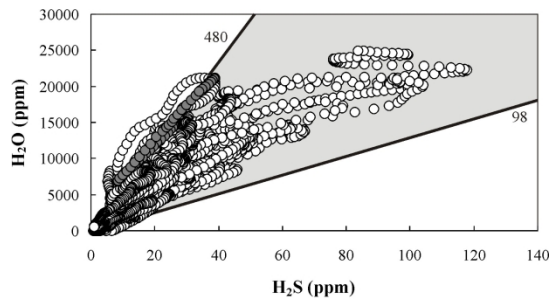


24°38'29"O

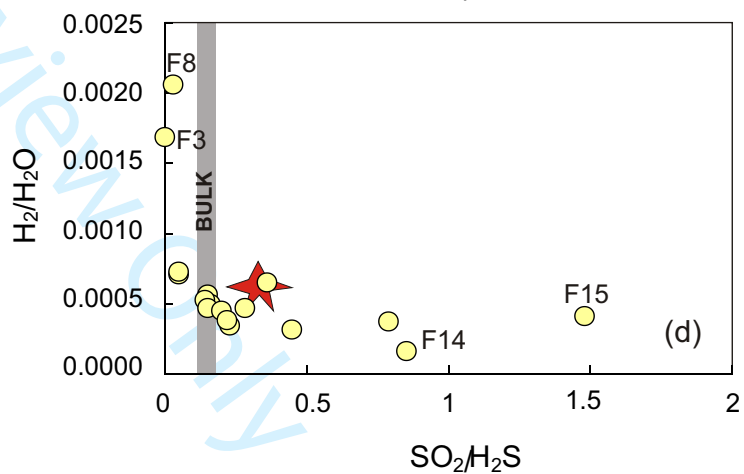
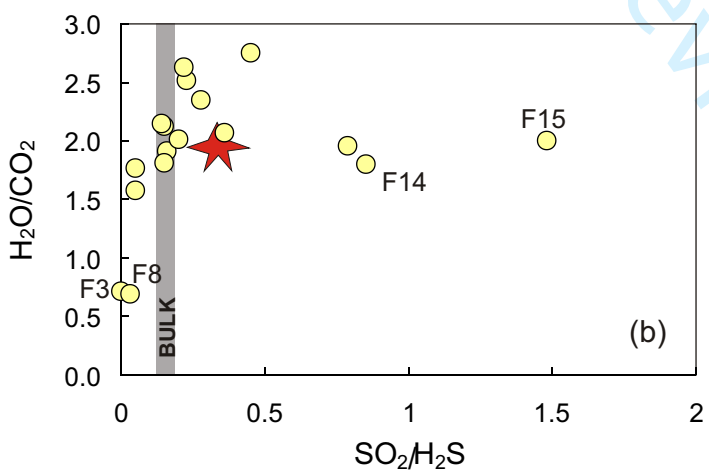
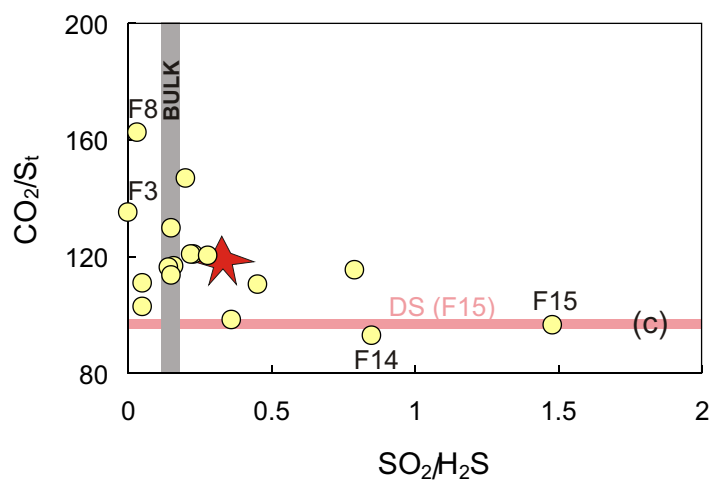
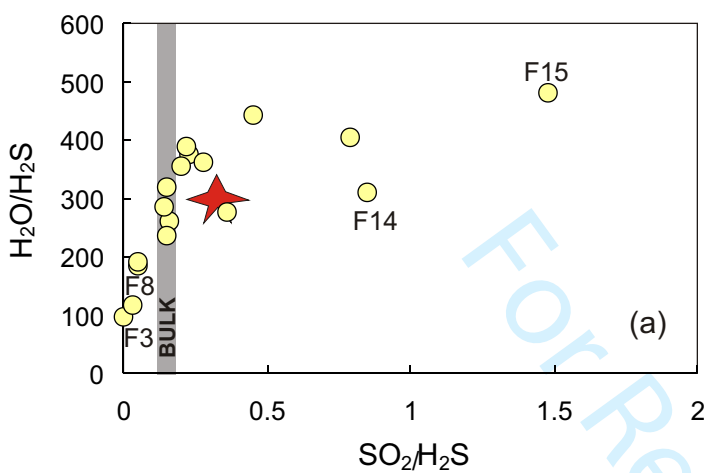
24°07'50"O

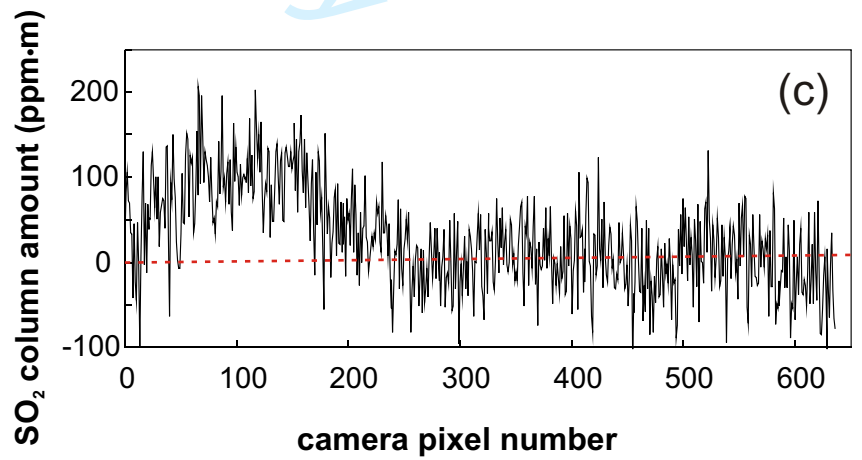
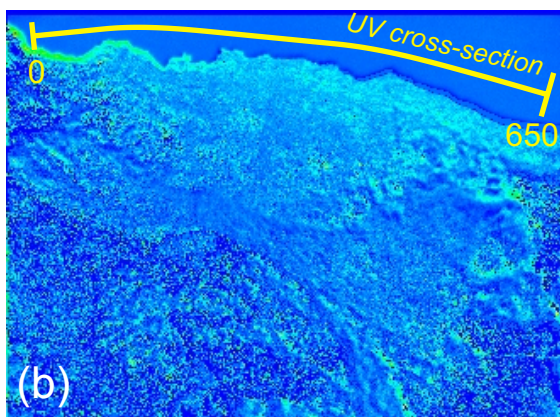
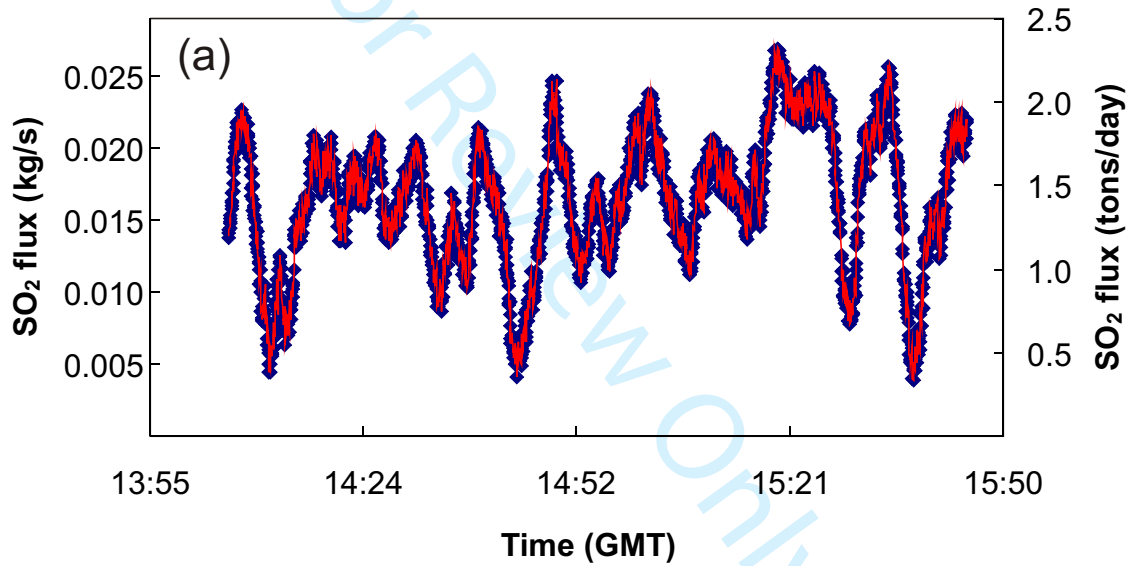


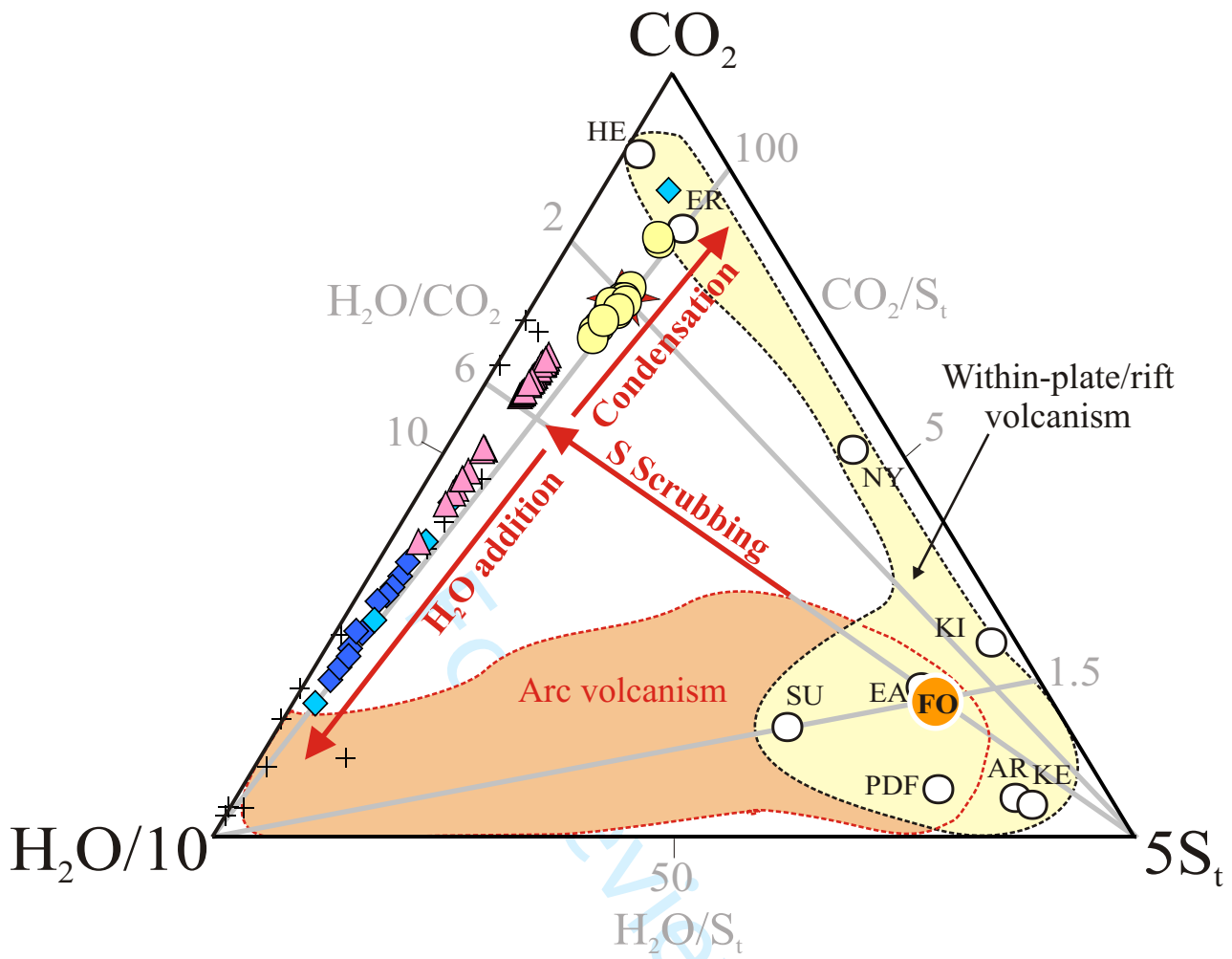
1
2
3
4
5
6
7
8
9
10
11
12
13
14
15
16
17
18
19
20
21
22
23
24
25
26
27
28
29
30
31
32
33
34
35
36
37
38
39
40
41
42
43
44
45
46
47
48
49
50
51
52
53
54
55
56
57
58
59
60



143x319mm (300 x 300 DPI)







- Pico do Fogo summit fumaroles (this study)
- Fogo eruptive plume gas (Hernández et al., 2015)
- ★ Mean (Pico do Fogo) (this study)
- △ Canary (Teide) (Melian et al., 2012)
- ◆ Azores (Caliro et al., 2015)
- ◆ Azores (MARES Project, this study)
- Magmatic gases (intraplate/rift) (Aiuppa, 2015)
- + Hydrothermal gases (Chiodini and Marini, 1998)

